Neoproterozoic glaciation on a carbonate platform margin in Arctic Alaska and the origin of the North Slope subterrane

Francis A. Macdonald†
Department of Earth and Planetary Sciences, Harvard University, 20 Oxford Street, Cambridge, Massachusetts 02138, USA

William C. McClelland
Department of Geological Sciences, University of Idaho, Moscow, Idaho 83843, USA

Daniel P. Schrag
Department of Earth and Planetary Sciences, Harvard University, 20 Oxford Street, Cambridge, Massachusetts 02138, USA

Winston P. Macdonald
Biology Department, Boston University, 5 Cummington Street, Boston, Massachusetts 02215, USA

ABSTRACT

The rotation model for the opening of the Canada Basin of the Arctic Ocean predicts stratigraphic links between the Alaskan North Slope and the Canadian Arctic islands. The Katakturuk Dolomite is a 2080-m-thick Neoproterozoic carbonate succession exposed in the northeastern Brooks Range of Arctic Alaska. These strata have previously been correlated with the pre–723 Ma Shaler Supergroup of the Amundson Basin. Herein we report new composite $\delta^{13}C$ profiles and detrital zircon ages that test this connection. We go further and use stratigraphic markers and a compilation of $\delta^{13}C$ chemostratigraphy from around the world, tied to U-Pb ages, to derive an age model for deposition of the Katakturuk Dolomite. In particular, we report the identification of ca. 760 Ma detrital zircons in strata underlying the Katakturuk Dolomite. Moreover, a diamictite present at the base of the Katakturuk Dolomite is capped by a dark-colored limestone with peculiar roll-up structures. Chemostratigraphy and lithostratigraphy suggest this is an early-Cryogenian glacial diamictite-cap carbonate couplet and that deposition of the Katakturuk Dolomite spanned much of the late Neoproterozoic. Approximately 500 m above the diamictite, a micropeloidal dolomite, with idiosyncratic textures that are characteristic of basal Ediacaran cap carbonates, such as tubestone stromatolites, giant wave ripples, and decameters of pseudomorphosed former aragonite crystal fans, rests on a silicified surface. Chemostratigraphic correlations also indicate a large increase in sedimentation rate in the upper ~1 km of the Katakturuk Dolomite and in the overlying lower Nanook Limestone. We suggest that the accompanying increase in accommodation space, along with the presence of two low-angle unconformities within these strata, are the product of late Ediacaran rifting along the southern margin of the North Slope subterrane. There are no strata present in the Amundson Basin that are potentially correlative with the late Neoproterozoic Katakturuk Dolomite, as the Cambrian Saline River Formation rests on the ca. 723 Ma Natkusiak Formation. Detrital zircon geochronology, chemostratigraphic correlations, and the style of sedimentation are inconsistent with both a Canadian Arctic origin of the North Slope subterrane and a simple rotation model for the origin of the Arctic Ocean. If the rotation model is to be retained, the exotic North Slope subterrane must have accreted to northwest Laurentia in the Early to Middle Devonian.

Keywords: Neoproterozoic, snowball Earth, cap carbonates, Arctic Alaska terrane, Katakturuk, Nanook, chemostratigraphy, detrital zircon geochronology, carbon isotope, oxygen isotope, glaciation.

INTRODUCTION

In his Alaskan orocline hypothesis, Sam Carey proposed that the Arctic Ocean opened as a sphenochasm complementary to the oroclinal bend of the northernmost Cordillera (Carey, 1955, 1958). This was later refined to the rotation model, which called for a Cretaceous 66° counterclockwise rotation of the Arctic Alaska–Chukotka Plate (Fig. 1) away from the Canadian Arctic islands about a pole in the Mackenzie River Delta (Hamilton, 1970; Grantz et al., 1979). While this model is the most widely accepted (for a review of the models, see Lawver and Scotese, 1990), the tectonic movements that precipitated the opening of the Arctic Basin remain controversial (Lane, 1997). This uncertainty is due in large part to the paucity of magnetic anomalies in the Canada Basin, since much of the ocean crust was formed during the Cretaceous Long Normal Interval (Sweeney, 1985). Moreover, paleomagnetic constraints are complicated by pervasive mid-Cretaceous overprints in the Brooks Range (Hillhouse and Grommé, 1983). Yet all is not lost, for Neoproterozoic and Paleozoic sequences on the Arctic margins provide geologic tests of the rotation model.

The Katakturuk Dolomite is a 2080-m-thick Neoproterozoic carbonate succession exposed in the northeastern Brooks Range of Arctic Alaska (Fig. 1). The rotation model predicts that these strata are a northern extension of pre–723 Ma "Succession B" intracratonic deposits of northwestern Laurentia (Rainbird et al., 1996), such as the Shaler Supergroup of Victoria Island (Young, 1981), the Little Dal Group in the Mackenzie Mountains (Aitken, 1981), and the Lower Tindir Group of Yukon-Alaska border area (Young, 1982). Herein we report lithostratigraphic, chemostratigraphic, and geochronologic studies that test both this correlation with Laurentian strata and the rotation model for the opening of the Arctic Ocean.

†E-mail: fmacdon@fas.harvard.edu

GSA Bulletin; March/April 2009; v. 121; no. 3/4; p. 448–473; doi: 10.1130/B26401.1; 14 figures; Data Repository item 2008190.

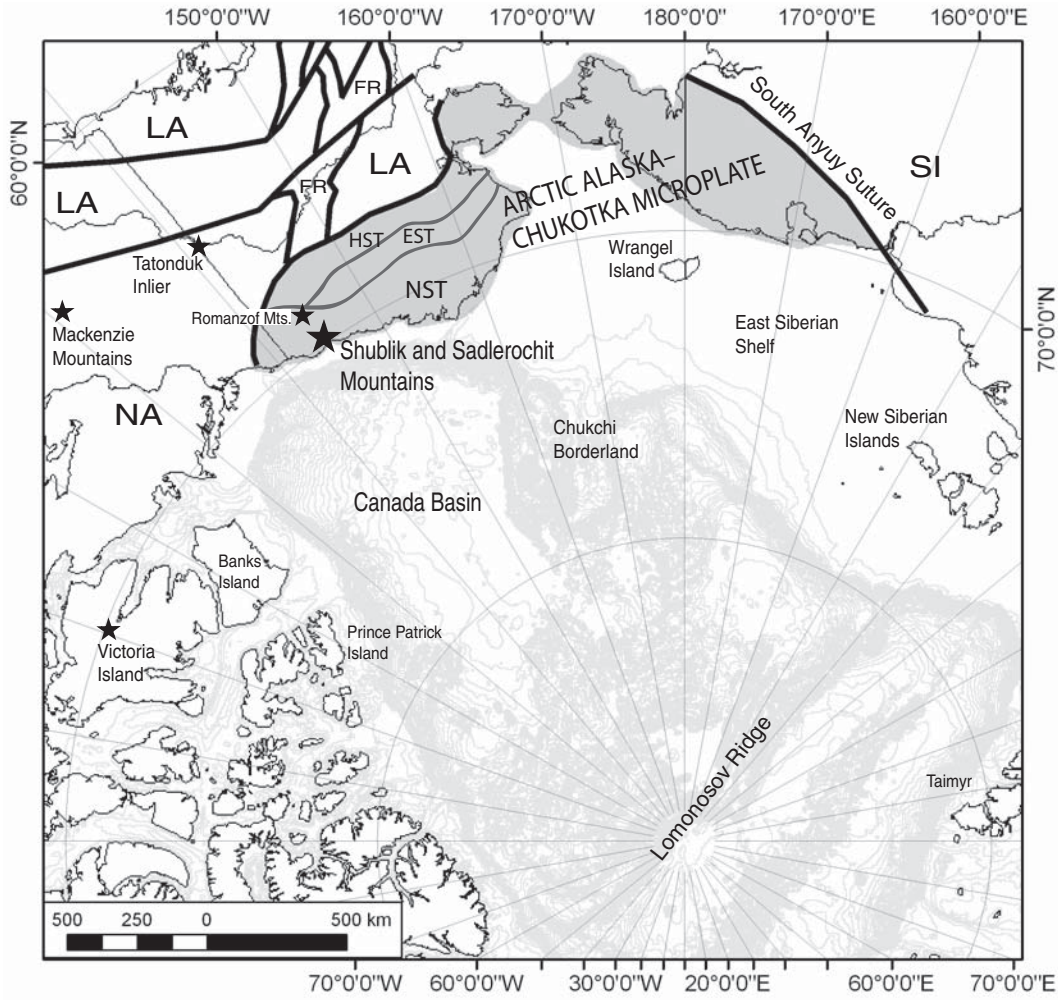

Figure 1. Location and tectonic map superimposed on the bathymetry of the Arctic Ocean, modified and simplified from Johnston (2001), Moore et al. (1994), Persits and Ulmishek (2003), and Colpron et al. (2007), with the Arctic Alaska–Chukotka microplate shaded gray. Abbreviations for terranes and subterranes: the North Slope subterrane (NST), the Endicott Mountains subterrane (EST), the Hammond subterrane, including the Angayucham, Coldfoot, De Long Mountains, Slate Creek subterranes (HST); FR—Farewell-Ruby terranes; NA—ancestral North America; LA—late accreted terranes; SI—Siberia. Stars are locations addressed in the text and Figure 14.

Furthermore, a redefinition of the age of the Katakturuk Dolomite integrates this sequence into our understanding of environmental change in the terminal Neoproterozoic.

Neoproterozoic strata contain evidence of multiple low-latitude glaciations (Harland, 1964; Hambrey and Harland, 1981; Evans, 2000), the breakup of Rodinia and assembly of Gondwanaland (Hoffman, 1991), the putative oxygenation of the deep oceans (Logan et al., 1995; Rothman et al., 2003; Fike et al., 2006), several high-amplitude carbon-isotope excursions (Knoll et al., 1986; Burns and Matter, 1993; Halverson et al., 2005), the acanthomorphic acritarch radiation (Grey et al., 2003; Grey, 2005), the rise and fall of the Ediacaran fauna (Glaessner and Wade, 1966; Cloud and Glaessner, 1982), and the advent of bilaterians and calcifying metazoans (Grotzinger et al., 1995; Fedonkin and Waggoner, 1997; Martin et al., 2000). However, both relative and absolute age uncertainties preclude a better understanding of the origins and interrelationships of these events. In order to bridge this gap, integrated, high-resolution studies of Late Neoproterozoic–Cambrian successions are necessary, and where possible, new sections need to be added to the record of this tumultuous period.

BACKGROUND

Neoproterozoic Carbon-Isotope Chemostratigraphy

Carbon-isotope records from marine carbonate strata are widely used for global stratigraphic correlation (Knoll et al., 1986; Saltzman et al., 2000; Halverson et al., 2005) and for studying the interplay between climate and biogeochemical cycling (Summons and Hayes, 1992; Zachos et al., 2001; Saltzman, 2005). Carbonate carbon isotopes are a particularly valuable proxy in the Neoproterozoic because of their resistance to alteration (Banner and Hanson, 1990; Veizer et al., 1999), the relative lack of calibrated biostratigraphy (Knoll and Walter, 1992), and the unique isotopic variability of the era (Kaufman and Knoll, 1995; Halverson et al., 2005). Carbon-isotope records have played a central role in studies of Neoproterozoic climate extremes (Hoffman and Schrag, 2002), ocean carbon dynamics (Rothman et al., 2003; Hotinski et al., 2004), carbonate production (Bartley and Kah, 2004), and the end-Neoproterozoic extinction event (Amthor et al., 2003).

The Neoproterozoic represents one of only two periods in Earth history (the other being 2.0–2.2 Ga) when the $\delta^{13}C$ of carbonates deviates strongly from 0 to 3‰ for long periods (Shields and Veizer, 2002), hovering around 5‰ for most of a 300-m.y. interval (Halverson et al., 2005). From this heavy baseline, there are several sharp, global, negative carbon-isotope excursions. The Rasthof (Yoshioka et al., 2003), Trezona (McKirdy et al., 2001; Halverson et al., 2002), and Maieberg (Kaufman and Knoll, 1995; Kennedy, 1996; Hoffman et al., 1998b) isotope excursions are intimately associated with Neoproterozoic glaciations. A pronounced

carbon-isotope excursion also occurs in the thin carbonate above the ca. 582 Ma Gaskiers glacial diamictites (Myrow and Kaufman, 1999; Bowring et al., 2003); however, the relationship between the Shuram excursion (Burns and Matter, 1993; Pell et al., 1993; Urlwin et al., 1993) and glaciation is unclear (Condon et al., 2005; Halverson et al., 2005). After the Shuram excursion, $\delta^{13}C$ values return to a 0‰–3‰ baseline, interrupted by the Precambrian-Cambrian boundary excursion (Amthor et al., 2003). When taken in geological context, with an eye for alteration and major hiatuses, these distinct isotopic anomalies and intervals permit robust stratigraphic correlations where paleontological constraints are scant.

Geological Background

The Neoproterozoic Katakturuk Dolomite and Cambrian-Ordovician Nanook Limestone form the backbone of the Shublik and Sadlerochit Mountains of the northeastern Brooks Range (Dutro, 1970). The Katakturuk Dolomite is also exposed to the southeast near Kikitak Mountain, with possible deep-water correlatives in the Third and Fourth Ranges (Fig. 2) and to the east between the Aichilik and Kongakuk Rivers (Reiser, 1971). Present exposures are the product of Paleogene north-vergent thrusting (Wallace and Hanks, 1990) related to accretion of the Yakutat block in southern Alaska (Moore et al., 1997; Fuis et al., 2008).

Anatomy of the Arctic Alaska–Chukotka Microplate

The Arctic Alaska–Chukotka microplate is a composite block of Alaskan subterranes that occupy the Brooks Range, the North Slope, and the Seward Peninsula (Fig. 1), along with the portion of the Chukotka Peninsula of Siberia that lies northeast of the South Anyuy suture zone (Churkin and Trexler, 1980; Rowley and Lottes, 1988; Miller et al., 2006). Some authors also combine the Arctic Alaska–Chukotka microplate with the Wrangel and New Siberian Islands and submerged continental crust in the Arctic to form the hypothetical Arctidia continent (Zonenshain et al., 1990; Sengor and Natal'in, 1996). The Alaskan portion of the Arctic Alaska–Chukotka microplate consists of, from the autochthon in the north to allochthonous sections south, the North Slope subterrane, the Endicott Mountains subterrane, the Hammond subterrane (including the Coldfoot, De Long Mountains, and Slate Creek subterranes), and the Angayucham subterrane (Moore et al., 1994). While it is generally assumed that the Arctic Alaska–Chukotka microplate is a fragment of continental crust, crystalline basement has only been identified in the Hammond subterrane and the Seward Peninsula, which are cored with Neoproterozoic orthogneiss (Patrick and McClelland, 1995). The "basement" of the North Slope subterrane is composed of the phyllite and quartzite of Old Grungy Mountain (Reiser et al., 1980) and the presumed Neoproterozoic equivalent in the Sadlerochit Mountains (Robinson et al., 1989), which underlies the Mount Copleston volcanics (Moore, 1987) and the Katakturuk Dolomite. The oldest rocks that have been identified in the Endicott Mountains subterrane are middle Paleozoic siliciclastic rocks, while the Angayucham subterrane is underlain by late Paleozoic-Mesozoic volcanics (Moore et al., 1994).

The North Slope subterrane is also distinguished from the other Arctic Alaska–Chukotka microplate subterranes in having experienced Silurian–Early Devonian deformation (Sweeney, 1982). Pre-Mississippian deformation appears to have been south-vergent (Oldow et al., 1987) and did not affect the Doonerak fenster or any of the other Arctic Alaska–Chukotka microplate terranes (Julian and Oldow, 1998), yet the tectonic origin of this contractional event has not been established (Moore et al., 1994). Furthermore, the North Slope subterrane and the rest of the Arctic Alaska–Chukotka microplate are separated by early Paleozoic ocean-island basalts in the Franklin Mountains (Moore, 1987) and arc volcanics in the Doonerak fenster (Julian and Oldow, 1998). A suture between the North Slope subterrane and the rest of the Arctic Alaska–Chukotka microplate may be marked by low-amplitude magnetic anomalies in the southern North Slope (Grantz et al., 1991), and by a change in the aeromagnetic and gravity fabrics across the southern margin of the North Slope subterrane (Saltus and Hudson, 2007). The age of this putative suture and to what degree the Arctic Alaska–Chukotka microplate subterranes have a shared Neoproterozoic and Paleozoic history are unclear. Equivalents of the Endicott Group and Carboniferous-Permian carbonates of the overlying Lisburne Group have been identified on the North Slope, Endicott Mountains, and Hammond subterranes, suggesting that these pieces had amalgamated by at least the late Paleozoic on a south-facing (present coordinates) passive margin (Moore et al., 1994).

The Brookian Orogeny began in the Late Jurassic and Early Cretaceous with the accretion of Paleozoic and Mesozoic seamounts and arcs, including the Angayucham terrane, on the southern margin of the Arctic Alaska–Chukotka microplate (Mayfield et al., 1988). Meanwhile on the northern margin, many of the models for the opening of the Arctic call for contemporaneous Early Cretaceous rifting (Grantz and May, 1983). Deformation progressed from south to north in the Arctic Alaska–Chukotka microplate culminating in the northeastern Brooks Range with Paleogene north-vergent thrusting and a cumulative shortening of 46%–48% (Hanks, 1991).

Tectonic Models for the Opening of the Canada Basin

From its modern inception (Hamilton, 1970), the **rotation model** was developed with bathymetric data (Grantz et al., 1979; Grantz et al., 1998), the rift histories and stratigraphic similarities of late Paleozoic and Mesozoic strata in the Canadian Arctic and Arctic Alaska (Embry, 1989; Embry and Dixon, 1990; Toro et al., 2004), and the transform morphology of the Lomonosov Ridge (Cochran et al., 2006). Barring any earlier movement relative to Laurentia, this model would place the pre-Cretaceous Arctic Alaska–Chukotka microplate offshore of what is now Banks Island. Many of the studies in favor of the rotation model cite Lower Cretaceous paleomagnetic data (Halgedahl and Jarrard, 1987). These data are from a single site consisting of two wells, lack a paleomagnetic confidence test other than a statistically insignificant reversal test, and imply not only 105° (+49°/–43°) counterclockwise rotation, but also that these strata were deposited 12° (+5/–4) to the south relative to cratonic North America (Stone, 1989). A similar post-Cretaceous northward translation of ~10° has been documented elsewhere on the North Slope and northeastern Russia (Witte et al., 1987; Stone, 2004). Although the paleomagnetic data support a rotation, the data are only grossly compatible with the 66° rotation called for in the rotation model. Moreover, a 66° rotation of the Arctic Alaska–Chukotka microplate is not geometrically feasible as it requires as much as 600 km of overlap of the Chukchi Borderland and East Siberian continental shelf onto the Canadian Arctic Islands, which is more than can be accounted for by extension (Lane, 1997).

Lane (1997) pointed out additional geological inconsistencies with the rotation model, including incongruous ages of deformation and deposition, and proposed a **fixed model** pinning Arctic Alaska near its present position (see also Lane, 1998). This model is not far removed from the Arctic-Alaska transform models that site the morphology of the Chukchi Borderland and vague magnetic lineation as evidence for rifting perpendicular to the northern margin of Alaska (Vogt et al., 1982). The fixed model also addresses the problem of a northern source of sediments on the North Slope subterrane by placing the submerged

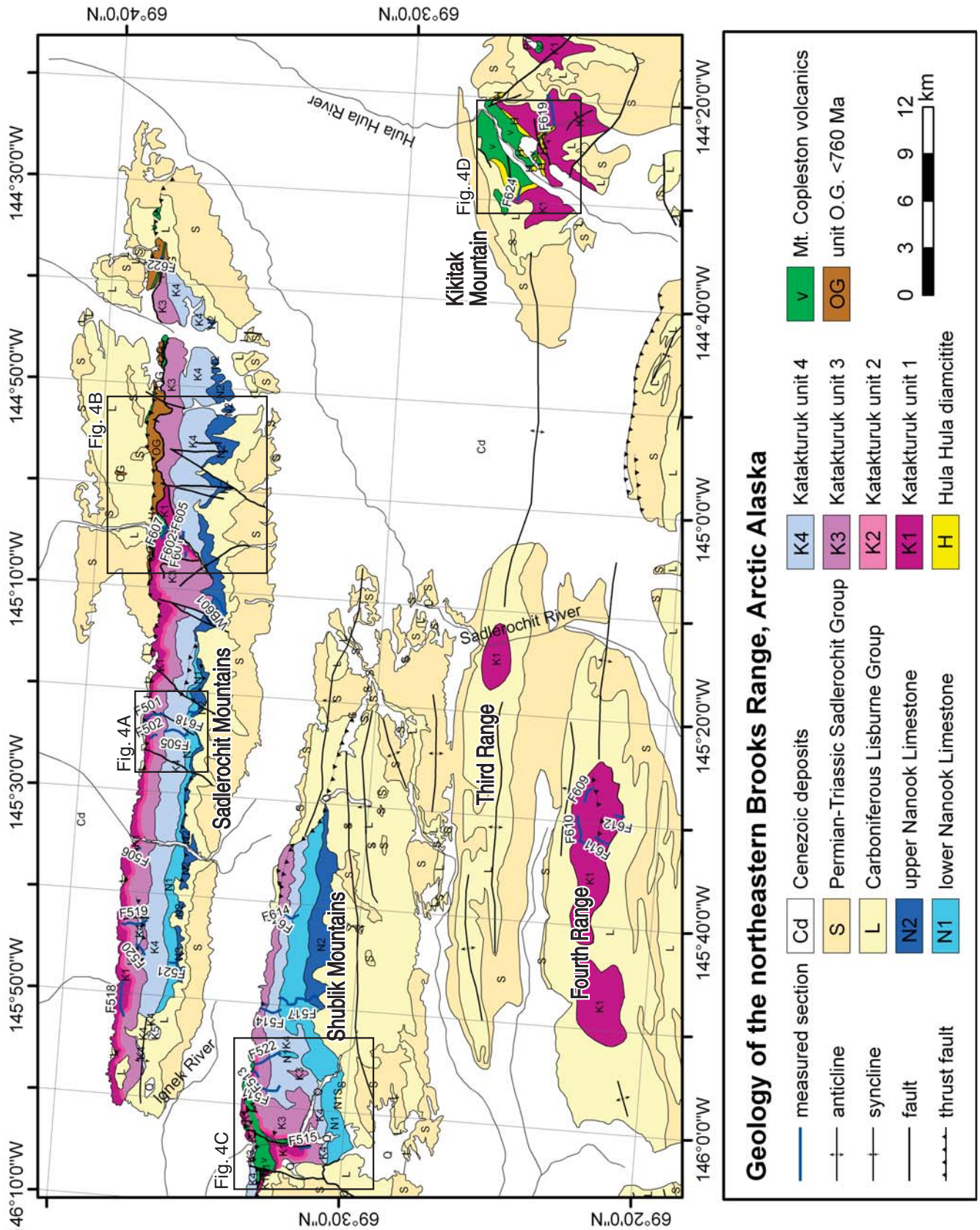

Figure 2. Geology of the Sadlerochit, Shublik, and Kikitak Mountains, and the Fourth Range. Post-Cambrian geology modified from Bader and Bird (1986) and Robinson et al. (1989).

continental crust of the Chukchi Borderland to the north of the present margin. However, fixist models, like the rotation model, fail to account for growing paleontological evidence of Siberian Paleozoic fauna in Alaskan terranes (Blodgett et al., 2002; Dumoulin et al., 2002).

Alternatively, many have supported the **Lomonosov rifting model** (Ostenso, 1974; Dutro, 1981; Kerr, 1981; Smith, 1987), which posits that the Arctic Alaska–Chukotka microplate originated near the Taimyr Peninsula of Russia. Considering the aforementioned problems with the paleomagnetic evidence, the strongest remaining argument against a Lomonosov rifting model is the transform morphology of the Lomonosov Ridge (Cochran et al., 2006). Most recently, citing detrital zircon provenance data, Miller et al. (2006) suggested a hybrid between the rotation and Lomonosov rifting models with differential motion between the Alaskan and Siberian portions of the Arctic Alaska–Chukotka microplate.

From a Cordilleran perspective, Johnston (2001) proposed that Arctic Alaska is part of a ribbon continent called SAYBIA (Siberia-Alaska-Yukon–British Columbia) that rifted off of Laurentia in the Cambrian, and accreted to the Arctic margin in an oroclinal orogeny. The **SAYBIA hypothesis** accounts for the post-Cretaceous northward translation of the Arctic Alaska–Chukotka microplate (Witte et al., 1987; Stone, 2004), geological differences between Arctic Alaska and the Canadian Arctic Islands (Lane, 1997), the presence of peri-Siberian Paleozoic fauna (Blodgett et al., 2002; Dumoulin et al., 2002), and possibly differences between terranes within the Arctic Alaska–Chukotka microplate through oblique sutures. In terms of the origin of the Arctic, the SAYBIA hypothesis is an extension of the Jones (1980) model calling for a southern provenance of the Arctic Alaska–Chukotka microplate. However, more recent iterations of the SAYBIA hypothesis do not include the North Slope subterrane in the Arctic Alaska–Chukotka microplate, suggesting a Cretaceous suture in the Brooks Range and a fixist model for the opening of the Arctic Ocean (Johnston, 2008).

These models each have different, testable implications for the Neoproterozoic and Paleozoic strata of Arctic Alaska.

STRATIGRAPHY

The pre-Mississippian stratigraphy of the northeastern Brooks Range has been described through paleontological reconnaissance (Dutro, 1970), geologic mapping (Leffingwell, 1919; Reed, 1968; Reiser, 1971; Robinson et al., 1989), and sequence analysis (Clough and Goldhammer, 2000), but no previous chemostratigraphic studies have been undertaken. Departing from the Robinson et al. (1989) lithostratigraphic division for the Katakturuk Dolomite, we have redefined the map units to highlight major sequence boundaries that represent depositional hiatuses (Figs. 2 and 3; supplementary data, GSA Data Repository Table DR4[1]). The goal is to separate units as time packets of nearly continuous deposition. The carbon and oxygen profiles through the Katakturuk Dolomite can also be divided into four intervals that correspond with the new unit divisions (Fig. 3). An attempt has been made to retain the naming scheme of Robinson et al. (1989) where possible, but within the new age constraints, several new names were needed.

Pre-Katakturuk Strata

The Neruokpuk Schist and Unit O.G.

Leffingwell (1919) defined the Neruokpuk Schist as interlayered pre-Mississippian quartzite, siliceous phyllite, argillite, limestone, and shale that crops out near Lake Peters. This name was used for the sub-Katakturuk strata on recent maps of the northeastern Brooks Range (Robinson et al., 1989); however, this "grab bag" unit is problematic since the Neruokpuk of Canada also includes siltstone with Late Cambrian trilobites and a stratigraphy distinct from what is exposed in the Sadlerochit Mountains (Reiser et al., 1978; Robinson et al., 1989; Lane, 1991). In the adjacent Demarcation Point Quadrangle, the Neruokpuk Schist rests unconformably above unfossiliferous carbonates potentially equivalent to the lower Katakturuk Dolomite, which in turn unconformably overlie a package of volcanic and clastic rocks (Reiser et al., 1980). Thus, the sub-Katakturuk clastic rocks can potentially be correlated with the stratigraphically lowest map units (pCpq, pCsd, and pClb of Reiser et al., 1980), and are herein referred to, informally, as map unit O.G. (supplementary data, Table DR4 [footnote 1]).

In the Sadlerochit Mountains, unit O.G. consists of >400 m of recessive, isoclinally folded and cleaved argillite, siltstone, mudstone, and thin-bedded dolomite with interbeds 1 cm to 10 m thick of fine- to coarse-grained sandstone and quartzite. Primary structures (e.g., cross beds and ripple marks) are commonly preserved. Meter-scale isoclinal folds are refolded about closed to tight upright folds indicating at least two deformational events. Quartzite beds contain detrital zircons as young as 760 ± 11 Ma (see data below), providing maximum age constraints on the Mount Copleston volcanics and the Katakturuk Dolomite. The actual thickness of unit O.G. is unknown as the basal contact lies above a thrust fault and the upper contact is either tectonized (Fig. 2) or unconformably overlain by Mount Copleston volcanics (Robinson et al., 1989). Approximately five kilometers east of Kikitak Mountain unit, O.G. is ~100 m thick, schistose, and overlain by greenschist facies metavolcanic rocks.

Mount Copleston Volcanics

Moore (1987) informally referred to the volcanic rocks in the Shublik and Sadlerochit Mountains as the Mount Copleston volcanics. These rocks are stratigraphically equivalent to volcanics and volcaniclastics near Kikitak Mountain (Reiser et al., 1970), and possibly correlative with the volcaniclastic rocks of Redwacke Creek (pCv of Reiser et al., 1980). The Mount Copleston volcanics are rusty weathering, dark maroon to black and green tholeiitic basalts with chlorite, calcite, and zeolite amygdules that are 1–5 mm in diameter. In the western Shublik Mountains the basalt has a structural thickness of up to 450 m thick with m-scale individual flows, preserved pillows and pahoehoe textures, and common native copper. A stratigraphic thickness is difficult to determine due to structural repetitions. Along the Hula Hula River, the Mount Copleston volcanics are structurally ~500 m thick, are commonly greenstone, and are dominated by volcaniclastic rocks in the upper ~100 m (Fig. 4).

In the Sadlerochit Mountains, the Mount Copleston volcanics are up to 105 m thick. The basal contact with the underlying, polydeformed unit O.G. is locally tectonized and inferred as unconformable (Robinson et al., 1989; Clough and Goldhammer, 2000). The basalts appear little metamorphosed with minimal chlorite, 5- to 10-mm-long plagioclase lathes, and intact, spherical amygdules. Major element and rare-earth element (REE) analyses of the Mount Copleston volcanics suggest a continental affinity (Moore, 1987).

On the far eastern end of the range (Figs. 2 and 4B), a coarse diabase sill intrudes unit O.G. and is considered to be coeval with the basaltic flows (Moore, 1987; Clough et al., 1990). This sill has yielded a whole rock Rb/Sr age of 801 ± 20 Ma (Clough et al., 1990); however, this isochron age is inconsistent with new U/Pb ages on detrital zircons from the underlying strata (see below).

[1]GSA Data Repository Item 2008190, color versions of selected figures, table of regional stratigraphic nomenclature, carbon and oxygen isotope data tables and crossplots, U-Pb LA-ICP-MS and TIMS data tables, is available at www.geosociety.org/pubs/ft2008.htm. Requests may also be sent to editing@geosociety.org.

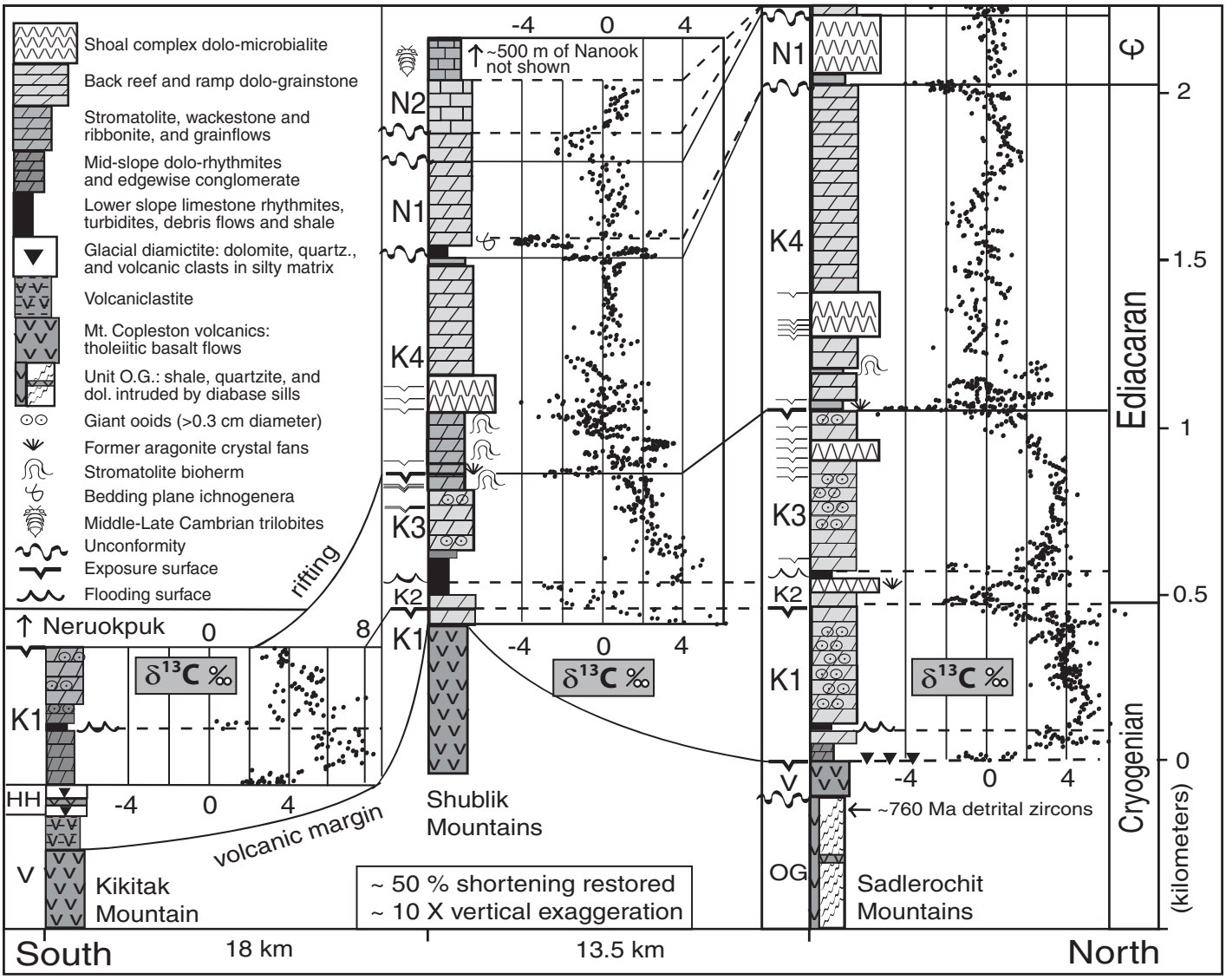

Figure 3. Composite carbon chemostratigraphy and lithostratigraphy of the Katakturuk Dolomite in the northeastern Brooks Range. Sadlerochit data from measured sections F501, F502, F505, F510, F602, F603, F604, F605, and F607; Shublik data from measured sections F513, F514, F517, F613, and F614; Kikitak data from measured sections F619 and F624 (see Fig. 2 for locations and supplementary data [footnote 1] for a color-coded figure showing the ties between sections). All carbonate carbon measurements in ‰ notation. Depositional distance between sections assumes 50% shortening (Hanks, 1991). Because these sections are composites, the lithofacies are generalizations of the dominant facies in that portion of the stratigraphy through multiple sections with interpretations of the depositional environment from the assemblage of facies.

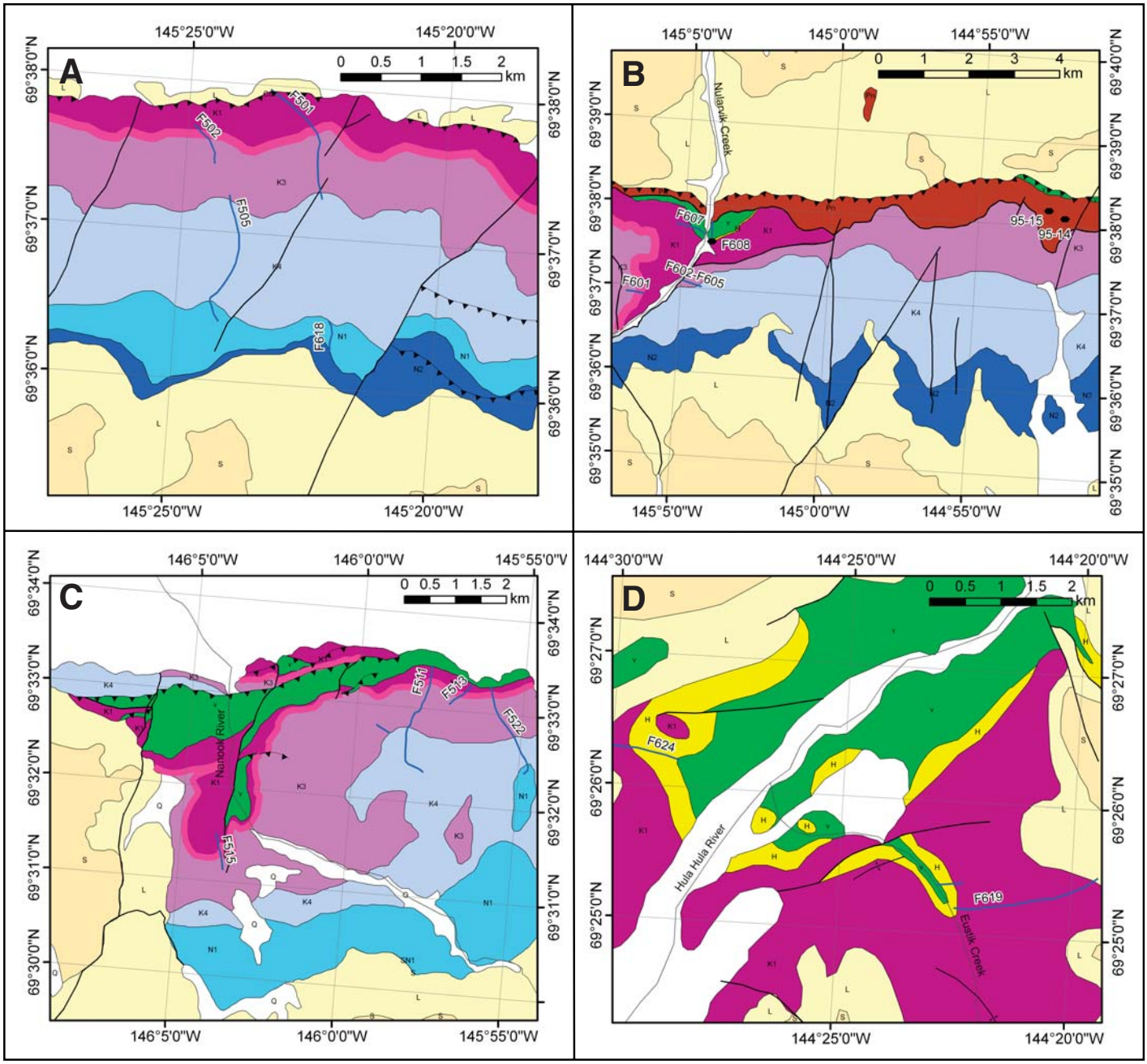

Figure 4. Geological maps with positions shown in Figure 2: (A) Central Sadlerochit Mountains; (B) Eastern Sadlerochit Mountains between Nularvik Creek and Itkilyariak River. Locations of detrital zircon samples are marked with hexagons; (C) Western Shublik Mountains along the Nanook River; (D) Kikitak Mountain along the Hula Hula River.

Hula Hula Diamictite

Reiser et al. (1970) first described the orange weathering diamictites along the Hula Hula River as carbonate debris flows with clasts of basalt, and included these deposits with the Katakturuk Dolomite. Herein we informally refer to these deposits as the Hula Hula diamictite. On the east side of the Hula Hula River, along Eustik Creek, the Hula Hula diamictite is ~50 m thick (Figs. 4D and 5). While incomplete exposure and structural repetition preclude the measurement of exact thicknesses, discrete outcrop-scale blocks allow confidence in the general stratigraphic relationships over tens of meters of stratigraphy. The lower 12 m of the diamictite is matrix-supported, with gravel- to cobble-sized clasts of orange dolomite, green to black basalts, and rare quartzite, in a green to tan siltstone matrix, and is interfingered with at least four basaltic flows that range in thickness from 2 to 0.2 m. The dolomite, quartzite, and siltstone are either from unit O.G. or are extra-basinal. The lower diamictite is overlain by ~30 m of poorly exposed, mm-laminated siltstone with rare gravel- and cobble-sized bedding-piercing lonestones (Fig. 6A) and multiple orange carbonate debris flows. The debris flows are distinguished from the diamictite in that the matrix and the clasts of the debris flows are of the same composition with no exotic clasts, and the clasts are tabular, sorted, and commonly imbricated. The upper 5 m of the Hula Hula diamictite are a massive, clast-supported diamictite with boulders of dolomite (up to 0.5 m across) and cobbles of basalt in a calcareous siltstone matrix. Because no faceted or striated clasts have been observed, a glacial origin is equivocal.

On the west side of the Hula Hula River near Kikitak Mountain, the basal Hula Hula consists of ~10 m of diamictite with cobbles of dolomite and basalt in a siltstone matrix, and an additional ~40 m of mm-laminated siltstone with lonestones and multiple orange carbonate debris flows. In the Kikitak Mountain area, the Hula Hula diamictite rests disconformably on the Mount Copleston volcanics. At this locality, the upper 50 m of the Mount Copleston volcanics consist of matrix-supported volcaniclastic diamictite of volcanic gravel and cobbles in a matrix of volcanic grit. It is unclear if this deposit is a debris flow or a glacial diamictite formed of reprocessed volcanics. We have included this deposit with the Mount Copleston volcanics rather than the Hula Hula diamictite because, unlike the overlying diamictite, it lacks foreign clasts.

In the eastern Sadlerochit Mountains, along the Nularvik Creek, the Hula Hula diamictite rests disconformably on pillow basalts of the Mount Copleston volcanics, along an erosive contact (Fig. 4B). At this locality, the diamictite is only 2 m thick and consists of angular cobbles of dolomite, quartzite, and basalt in coarse, clast-supported arkosic grit (Fig. 5).

Katakturuk Dolomite

The Katakturuk Dolomite was named by Dutro (1970) for its exposure in the Katakturuk River canyon in the Sadlerochit Mountains. Katakturuk is an English derivation of the Inupiaq word *Qattaqtuuraq,* which means "a wide open place" (Clough, 1989). The Katakturuk Dolomite has previously been identified at three localities: the Sadlerochit Mountains, the Shublik Mountains, and on both sides of the Hula Hula River near Kikitak Mountain (Clough and Goldhammer, 2000). Probable distal equivalents are present in the Third and Fourth Ranges (Fig. 2), and to the east in the Demarcation Point Quadrangle (Reiser et al., 1980).

Balanced cross-sections have suggested 46%–48% shortening in the northeastern Brooks Range fold-and-thrust belt (Hanks, 1991). This implies a pre-Mississipian distance between the Sadlerochit and Shublik Mountains of ~13.5 km, and an additional ~18 km to the Third Range, which is on the same thrust block as Kikitak Mountain (Fig. 2).

In the Sadlerochit Mountains, the Katakturuk Dolomite is ~2080 m thick, whereas it is only ~1200 m in the Shublik Mountains due to a basal truncation and the thinning of the upper ramp facies to the south. The reduced thickness of the Katakturuk Dolomite reported here (in contrast to the 2500 m thickness reported by Clough and Goldhammer, 2000) is due in part to our correlation of the upper ~250 m of the Katakturuk Dolomite in the Sadlerochit Mountains with the lower Nanook Limestone in the Shublik Mountains (supplementary data, Table DR4 [footnote 1]), but also, Clough and Goldhammer's (2000) thickness is from a composite section of both ranges. Near Kikitak Mountain, the Katakturuk Dolomite is only 458 m thick with the upper portion of the stratigraphy truncated by the sub-Mississippian unconformity.

Generally, the Katakturuk Dolomite is composed of massive, light-gray, shallow-water dolostones with common coated grains, stromatolites, and void-filling isopachous cement. Parasequences are distinguished by flat-bedded, micritic rhythmite shallowing upward progressively to differentially compacted ribbonite, and then above wave base to peritidal grainstone and microbialaminite. It is often difficult to determine what the grainstone clasts were composed of as the grainstones are commonly recrystallized, and consequently we herein refer to massive shallow-water carbonates generically as grainstones. Flooding surfaces are defined by an abrupt appearance of shale or marl, and exposure surfaces by irregular karstic dissolution surfaces or teepee structures (Kendall and Warren, 1987). To highlight the major unconformities and disconformities, we have divided the Katakturuk Dolomite into four informal units (see supplementary data, Table DR4 [footnote 1], for a comparison of the unit distinctions described here and those of previous workers).

Precambrian dolomites dominated by stromatolites and coated grains, potentially correlative with the Katakturuk Dolomite, have been described elsewhere on the Arctic Alaska–Chukotka microplate in the Hammond subterrane of central and western Brooks Range (Dumoulin, 1988; Dumoulin and Harris, 1994), and in the Farewell terrane (Babcock et al., 1994) of central Alaska; however, it is unclear if these terranes were attached to the Arctic Alaska–Chukotka microplate in the Neoproterozoic.

Unit K1

In the Sadlerochit Mountains, K1 is ~530 m thick, and is equivalent to Robinson et al.'s (1989) spire dolomite member and the lower ~30 m of the zebra dolomite member. The base of K1 is typically faulted out or covered in scree; however, in the eastern Sadlerochit Mountains along Nularvik Creek (Fig. 4B), the basal contact is exposed with the Hula Hula diamictite overlain by ~5 m of a variably dolomitized, dark limestone and an additional ~75 m of rhythmite interspersed with tabular clast carbonate breccias, which are interpreted as debris flows. These shallow upward to grainstone underlying a prominent flooding surface of marl and rhythmite at ~150 m above the Hula Hula diamictite. The rest of K1 consists of ~350 m of monotonous, massively bedded, often silicified grainstone and packstone containing giant ooids (~5 mm diameter). The last parasequence of K1 begins with rhythmite that, within 1 m, shallows upward into stromatolites and grainstone. This high-stand tract continues for another 30 m to the top of K1 and consists of resistant, heavily silicified grainstone with brecciated beds of recrystallized black chert that weather a distinct black and white.

In the Shublik Mountains, most of K1 is basally truncated, and only the last parasequence is present. It is difficult to determine the nature of the contact with the underlying Mount Copleston volcanics as it is covered in rubble. However, map relations indicate that the contact is parallel to bedding and the amount of K1 above the contact is consistent throughout the range (Fig. 4C).

Near Kikitak Mountain, the Katakturuk Dolomite is composed entirely of K1 and measures

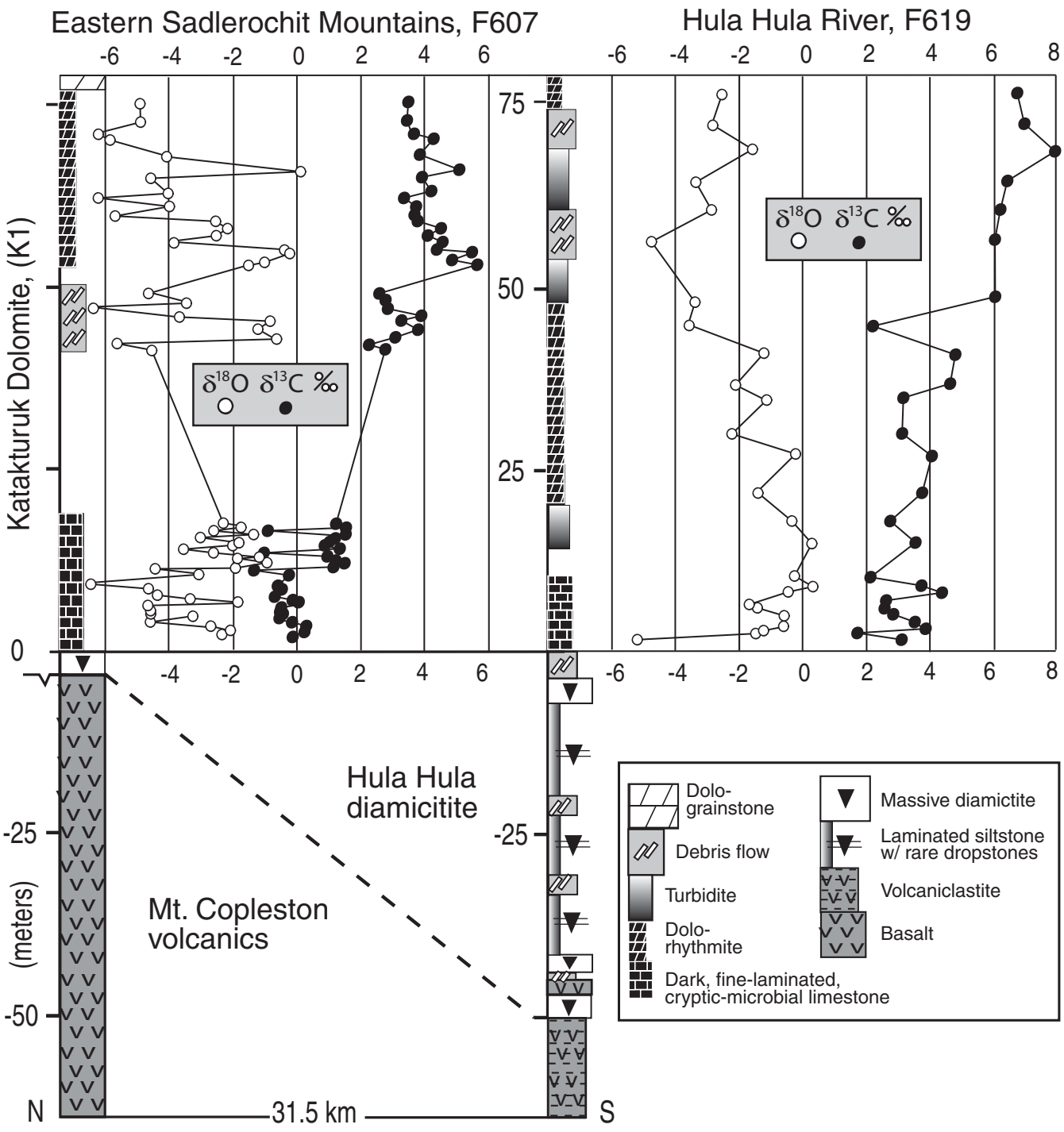

Figure 5. Stratigraphy of the Mount (Mt.) Copleston volcanics, the Hula Hula diamictite, and the lower portion of unit K1 along Nularvik Creek in the eastern Sadlerochit Mountains (section F607), and along the east side of the Hula Hula River (section F619). Carbon-isotope values are also shown for the lower portion of unit K1 on the west side of the Hula Hula River (section F624), where it is best exposed. Depositional distance between sections assumes 50% shortening (Hanks, 1991).

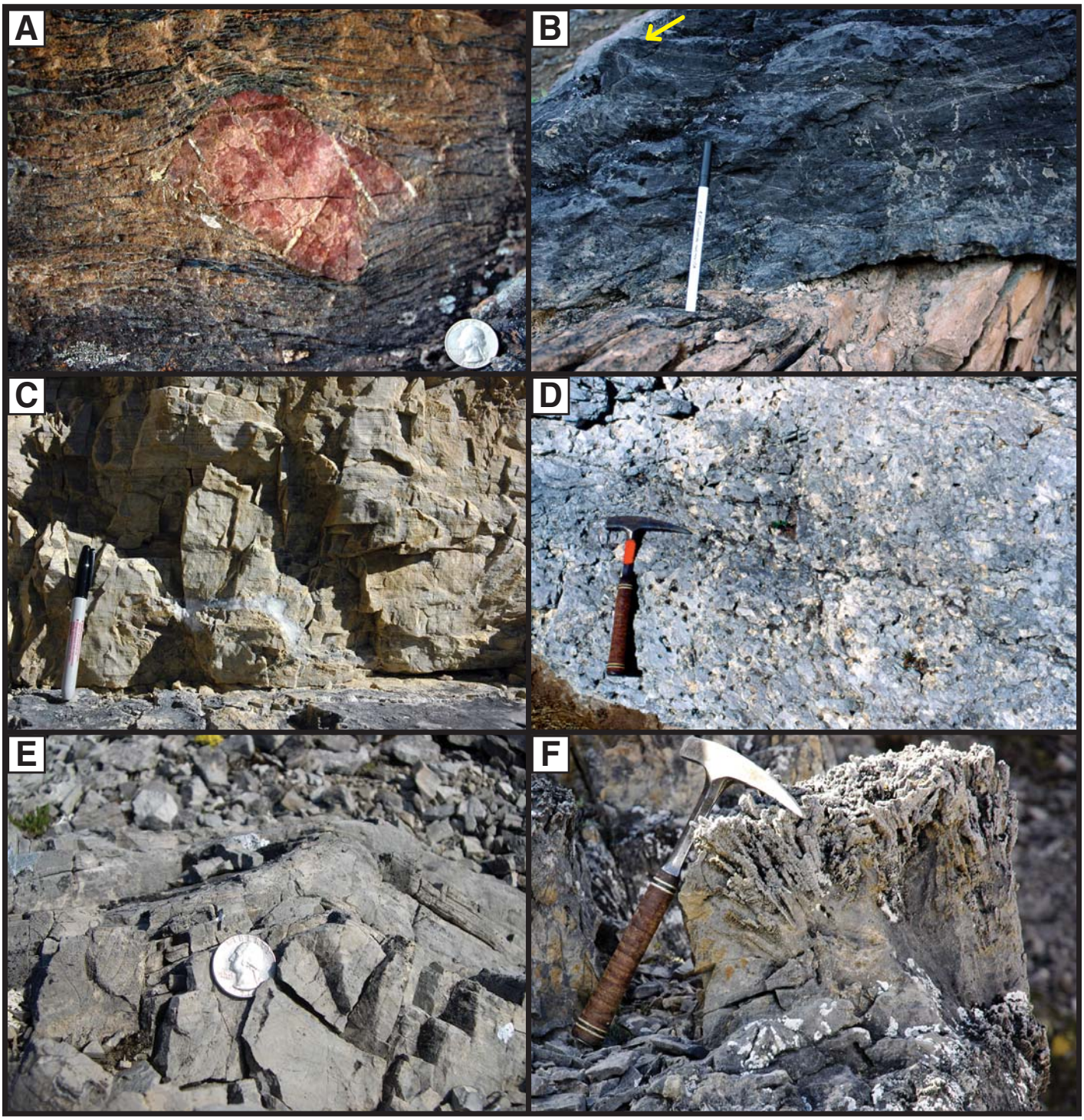

Figure 6. (A) Pink dolomite clast in a laminated siltstone matrix of the Hula Hula diamictite along Eustik Creek, section F619. Laminations are truncated on the right side of the clast, but are also compacted around and above the clast; (B) Knife-sharp contact between the Hula Hula diamictite and the Katakturuk Dolomite at Kikitak Mountain (section F624) with yellow arrow pointing at a roll-up structure; (C) Marker resting on knife-sharp basal contact of the Nularvik cap carbonate (unit K2), showing fine laminations and silica cements, along the Nularvik River in the Sadlerochit Mountains (section F601); (D) Plan view of tubestone stromatolite in the Nularvik cap carbonate in western Shublik Mountains (section F515). Pock marks reflect the recessive weathering of the cements that fill the cm-diameter tubes; (E) Wave ripples in central Sadlerochit Mountains (section F508); (F) Silicified crystal fans of unit K2 along the Nularvik River in the eastern Sadlerochit Mountains (section F601).

458 m thick; the upper Katakturuk Dolomite is truncated by the sub-Mississippian unconformity. Our lithostratigraphy and chemostratigraphy (Fig. 3) argue against previous correlations of these strata with unit K3 (Clough and Goldhammer, 2000). West of the Hula Hula River (F624, Fig. 4D), the Hula Hula diamictite is overlain in a knife-sharp contact by a black limestone with microbial "roll-up" structures (Fig. 5B), in which laminations are highly contorted despite the lack of evidence for exposure, tectonic folding, or synsedimentary slumping. Above this black microbialaminite is 180 m of rhythmite interspersed with tabular clast debris flows, an interval of 10 m of shale, and an additional 84 m of rhythmite, carbonate wackestone, and debris flows with clasts of silicified ooids. The upper ~175 m of K1 near Kikitak Mountain (F619, Fig. 4D) consists predominantly of peritidal, silicified, planar cross-bedded grainstone with giant ooids (Fig. 3).

In the Fourth Range, at least 1000 m of unfossiliferous, dark-colored limestone rhythmites and turbidites with minor shale and quartzite are exposed in the core of an anticline under the sub-Mississippian unconformity. Reiser (1971) reported a thickness of ~2100 m; however, it appears there is at least one major structural repetition within these strata. Similar lithologies have been described ~100 km to the east between the Aichilik and Kongakuk Rivers, and in the Third Range (Reiser, 1971; Reiser et al., 1980). Herein we use chemostratigraphic profiles and the regional stratigraphic architecture to argue that these strata are all deep-water facies of unit K1.

The Nularvik Cap Carbonate, Unit K2

The Nularvik cap carbonate (unit K2) is named informally after thick exposures that crop out on the west side of the Nularvik Creek in the eastern Sadlerochit Mountains. Measured sections of unit K2 vary in thickness from 50 to 147 m. The basal ~35 m of unit K2 is composed primarily of a buff-colored, hummocky-bedded, fine-laminated micropeloidal dolomite with low-angle cross stratification. The lower 15 m of these strata also contain funnel-shaped, isopachous calcite and silica cements (Fig. 6C). In the Sadlerochit Mountains, giant symmetrical wave ripples (Allen and Hoffman, 2005) are present in the top meter of the micropeloidal portion of K2. Individual crests have up to 18 cm of synoptic relief, with a crest-to-trough distance of 40 cm, and have yielded crestal azimuth orientations of 172° and 175° (n = 2). The wave ripples rest below a heavily silicified surface that is commonly brecciated (Fig. 6E). This surface is overlain with as much as 60 m of pseudomorphosed aragonite crystal fans, with individual fans measuring as tall as 60 cm (Fig. 6F). Although the matrix between the fans is massively recrystallized, inhibiting detailed petrographic analysis, truncation by overlying bedding indicates that fans are primary structures (Clough and Goldhammer, 2000). The crystal fans are also interbedded with grainstone, and with multiple horizons of teepee structures, which formed during subaerial exposure (Kendall and Warren, 1987).

In the western Shublik Mountains, the micropeloidal portion of K2 is less than 30 m thick, and the funnel-shaped isopachous cements can be followed laterally to "tubestone" stromatolite bioherms (Corsetti and Grotzinger, 2005) that measure as much as 8 m thick (Figs. 6D and 7). These stromatolites form very broad mounds that on an outcrop scale show no evidence of synoptic relief. The term "tubestone" refers to the irregularly spaced, cm-diameter columns of void-filling cement within the bioherms (Fig. 6D) that display inheritance over meters of stratigraphy. Crystal fans are not developed in the Shublik Mountains, but instead, unit K2 contains a single transgressive sequence from the basal micropeloidal dolomite, upward to dolo-ribbonite, limestone rhythmite, and shale.

Unit K3

In the Sadlerochit Mountains, unit K3 is ~500 m thick. The base is defined by a shale flooding surface that is commonly accompanied with tabular clast breccias, which are interpreted as debris flows. Above these breccias, unit K3 continues with ~50 m of well-defined, 5- to 10-m-scale parasequences. The middle ~400 m of K3 consists of a monotonous sequence of silicified, tabular cross-bedded grainstone and ooid grainstone that grade upward into a shoal complex composed of a series of thin parasequences defined by teepee structures and microbialaminates. The top of unit K3 is defined by a distinctive, laterally persistent, up to 10-m-thick karstic surface composed of a calcretized, vadose pisolite, with individual pisoids measuring over 1 cm in diameter.

In the Shublik Mountains, unit K3 begins with ~100 m of rhythmite, carbonate turbidite and tabular clast debris flows, constituting a major expansion of the thin shale that overlies unit K2 in the Sadlerochit Mountains. However, the overlying grainstones are thinner in the Shublik Mountains, measuring only 220 m. In the Shublik Mountains, the upper 20 m contain a spectacular branching stromatolite bioherm capped by the distinctive vadose pisolite marker bed (Fig. 8).

Unit K4

Unit K4 measures 980 m in the Sadlerochit Mountains and 650 m in the Shublik Mountains. The unit begins above the pisoidal karstic surface at the top of unit K3 with cm-scale pseudomorphosed aragonite crystal fans (Fig. 8) that are present in both the Sadlerochit and Shublik Mountains and persist for ~10 m of strata. The fans are in ribbonite beds at the base of an upward shallowing sequence that includes m-tall, elongate stromatolites and culminates in a distinctive brown grainstone and an exposure surface. Unlike other stromatolites in the Katakturuk Dolomite, this lowest stromatolite horizon in K4 shows no evidence of trapping and binding. The next parasequence begins with clotty bulbous stromatolites that persist for as much as 100 m of stratigraphic section. These stromatolites are developed primarily in a stromatolite clast wackestone and shallow up to a thick sequence of microbialaminite (~150 m) with multiple dissolution surfaces. Above the microbialaminite is another ~500 m of massive cross-bedded grainstone. In the Sadlerochit Mountains, unit K4 terminates with an additional ~270 m of grainstone with peculiar pink and white isopachous cements that have the appearance of dentures. These are possibly speliothems from overlying karstic surfaces.

The Nanook Limestone

The Lower Nanook Limestone (Unit N1)

The lower Nanook Limestone is best exposed in the Shublik Mountains, where it is 290 m thick (although greater thicknesses have been measured by Robinson et al., 1989). Despite the name, the lower Nanook Limestone is composed primarily of unfossiliferous, massively recrystallized dolomite grainstone. The only evidence of metazoan influence on the deposition of unit N1 is in the lowermost ~55 m, where carbonate-shale turbidites and rhythmites contain mm- to cm-wide, bed-parallel ichnogenera (Fig. 9; Clough and Goldhammer, 2000). Trace fossils of this size have only been observed in strata that are latest Ediacaran in age or younger (Crimes, 1992). These strata are overlain by ~235 m of massively bedded, white dolostone.

In the Sadlerochit Mountains, the lower Nanook Limestone has been previously mapped as the uppermost Katakturuk Dolomite (Robinson et al., 1989; Clough and Goldhammer, 2000), where it forms resistant ridgelines and is composed predominantly of massive, silicified cave breccias with dissolution features and microbialaminite with bird's-eye texture. This miscorrelation likely occurred because the distinct turbidites with ichnogenera are not present in the Sadlerochit Mountains (see Discussion).

The Upper Nanook Limestone (Unit N2)

The ~800-m-thick unit N2 unconformably overlies the lower Nanook Limestone on a

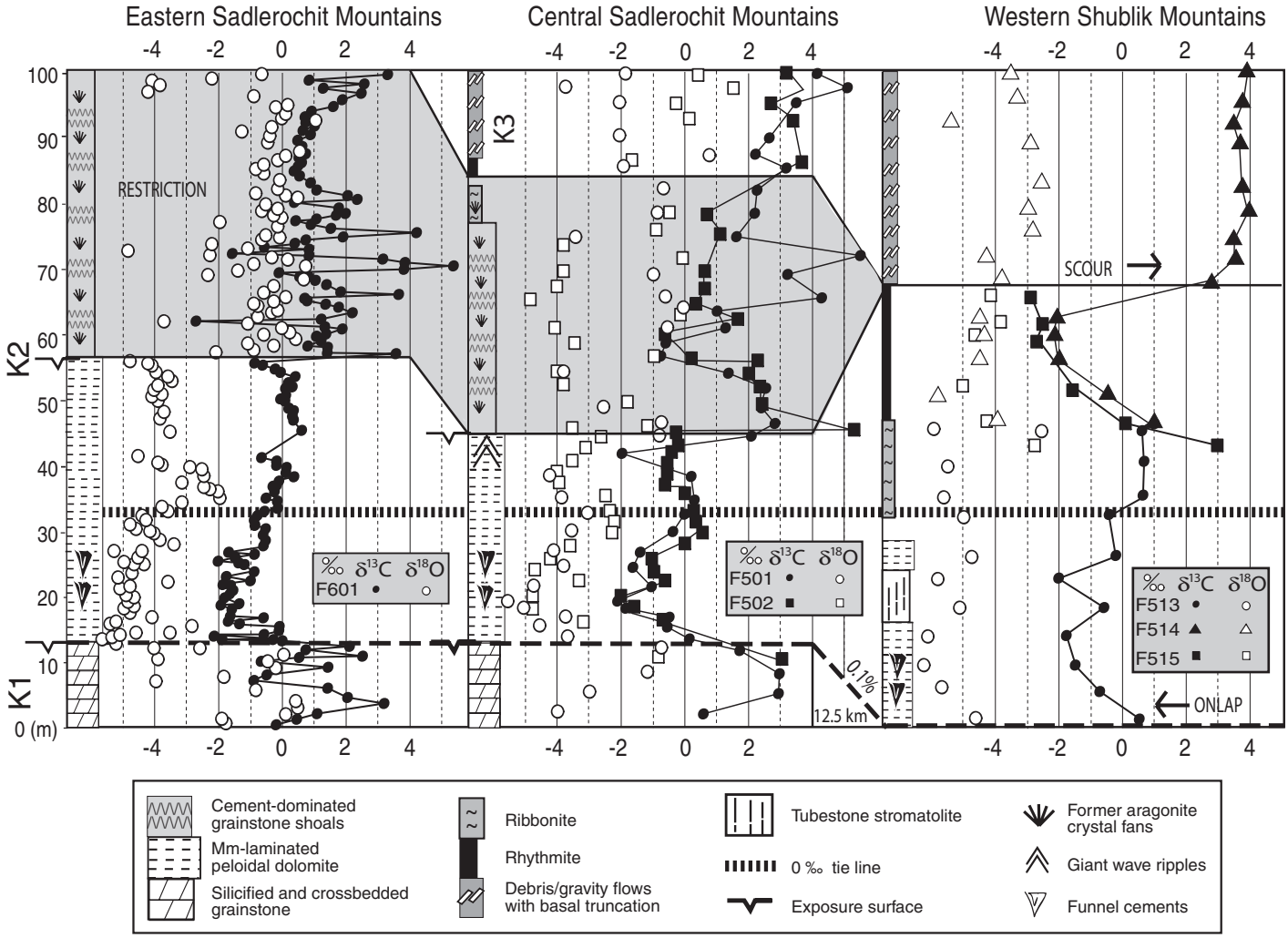

Figure 7. Chemostratigraphy and lithostratigraphy of the Nularvik cap carbonate (unit K2). See Figure 2 for locations of measured sections. All carbonate carbon (filled) and oxygen (hollow) measurements in ‰ notation. Stratigraphic log in central Sadlerochit Mountains from section F501, with section F502 carbon and oxygen data added. Stratigraphic log in western Shublik Mountains from F513 and F514 with F515 carbon and oxygen data added. Depositional distance between sections assumes 50% shortening (Hanks, 1991).

surface that is commonly silicified and brecciated. The upper Nanook Limestone begins with >100 m of massive dolomite grainstone with cement-filled vugs and minor limestone. These grainstones are overlain with ~160 m of peloidal limey packstones containing Middle to Late Cambrian trilobites with North American paleobiogeographic affinities (Blodgett et al., 1986), and an additional ~300 m of Lower Ordovician limestone grainstones that contain trilobites with affinities to the Bathyurid Province, which occupied low paleolatitude sites of North America, Greenland, northeastern Russia, and Kazakhstan (Whittington and Hughes, 1972; Blodgett et al., 1986). Conodonts in these strata show a cosmopolitan paleogeographic affinity (Dumoulin et al., 2002) and have a conodont alteration index of 4 (Harris et al., 1990). The upper Nanook Limestone terminates with ~160 m of Middle to Upper Ordovician strata, which contain pentamerid brachiopods that have a Siberian affinity (Blodgett et al., 2002). In the western Shublik Mountains, the Nanook Limestone is unconformably overlain by ~70 m of Early Devonian limestone (Blodgett et al., 1992), which are possibly foreland deposits.

CHEMOSTRATIGRAPHY

Sample Selection and Preparation

During our mapping, we collected samples for $\delta^{13}C$ and $\delta^{18}O$ analyses within measured stratigraphic sections. All samples were cut perpendicular to lamination, revealing internal textures. Between 5 and 20 mg of powder were micro-drilled from the individual laminations (where visible), with an eye to avoid veining, fractures, and siliciclastic components. All subsequent isotopic analyses were performed on aliquots of this powder.

Isotopic Analysis

Carbonate $\delta^{13}C$ and $\delta^{18}O$ isotopic data were acquired simultaneously on a VG Optima dual inlet mass spectrometer attached to a VG Isocarb preparation device (Micromass, Milford, Massachusetts) in the Harvard University Laboratory for Geochemical Oceanography. Approximately 1-mg microdrilled samples were reacted in a common, purified H_3PO_4 bath at 90 °C. Evolved CO_2 was collected cryogeni-

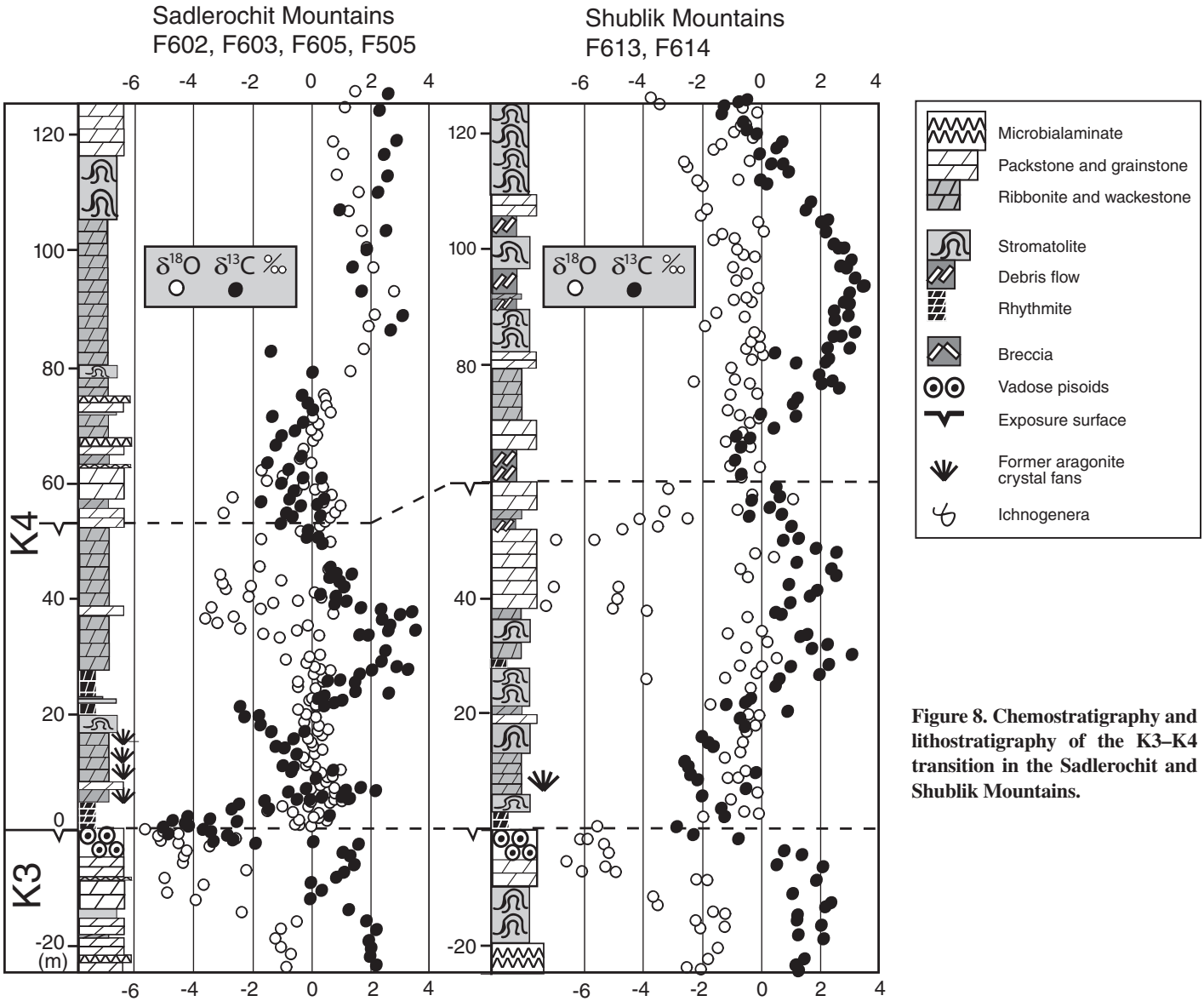

Figure 8. Chemostratigraphy and lithostratigraphy of the K3–K4 transition in the Sadlerochit and Shublik Mountains.

cally and analyzed using an in-house reference gas. External error (1σ) from standards was better than ±0.1‰ for both $\delta^{13}C$ and $\delta^{18}O$. Samples were calibrated to VPDB (Vienna Pee-Dee Belemnite) using the Cararra marble standard. Potential memory effect resulting from the common acid-bath system was minimized by increasing the reaction time to seven minutes for dolomite samples. Memory effect is estimated at <0.1‰ based on variability of standards run after dolomite samples. Carbon ($\delta^{13}C$) and oxygen ($\delta^{18}O$) isotopic results are reported in per mil notation of $^{13}C/^{12}C$ and $^{18}O/^{16}O$, respectively, relative to the standard VPDB. Herein we report $\delta^{13}C$ and $\delta^{18}O$ measurements of 2350 samples (see supplementary data [footnote 1]).

Results

Carbon-isotope profiles are broadly similar through the three ranges (Fig. 3). In the Sadlerochit Mountains, above the Hula Hula diamictite, in the basal 20 m of K1, $\delta^{13}C$ values rise from –2‰ to +6‰ (Fig. 5), and then for the rest of K1 range between +3‰ and +6‰. In the Kikitak Mountain area, $\delta^{13}C$ values rise from +1‰ to +8‰ and then oscillate around +5‰ with a bit more variability. Reconnaissance $\delta^{13}C$ analyses through potentially correlative limestones in the Fourth Range give values averaging ~+9‰ with values peaking above +12‰ (supplementary data tables [footnote 1]). The significance of these enriched values is discussed below. In the last parasequence of K1, values drop to 0‰.

Carbon-isotope profiles through K2 have a sigmoidal shape with a nadir at –2‰. In the Sadlerochit Mountains, $\delta^{13}C$ values are highly variable through the cement-dominated crystal fans of K2. In the Shublik Mountains, $\delta^{13}C$ values in the rhythmites at the top of K2 bottom out at –3‰, then jump to +3‰ in the overlying debris flows (Fig. 7). This abrupt change in isotopic values indicates that either section is missing at this contact.

Beginning with sediments deposited during the transgression overlying the crystal fans at the top of K2 in the Sadlerochit Mountains, $\delta^{13}C$ profiles display a smooth curve starting at +2‰, increasing to +4‰ and then diving to negative values in the pisolite-bearing beds at the top of K3 (Figs. 3 and 8). Unit K4 has $\delta^{13}C$ values that

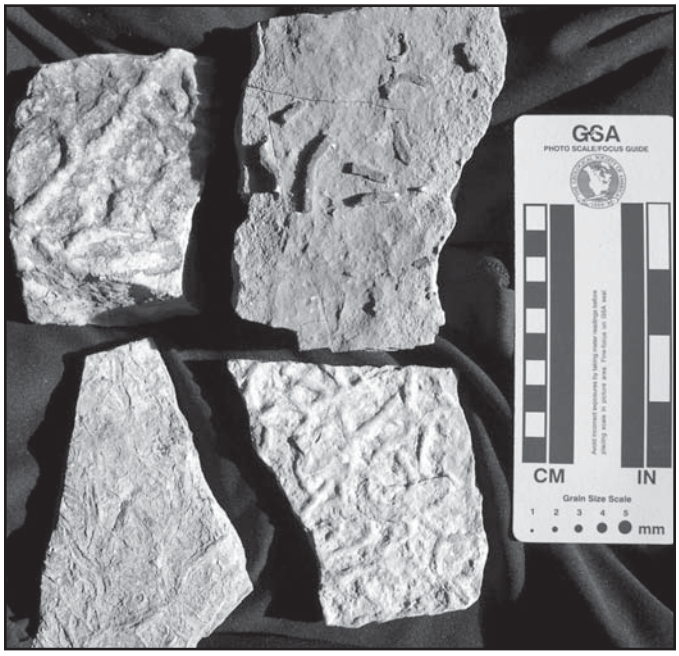

Figure 9. Ichnogenera from the lower Nanook Limestone in section F517. Samples were collected between 40 and 45 m above the base of unit N1.

begin at −5‰, rise to 0‰ before another negative anomaly to −2‰, then rise again to +4‰ before oscillating around zero (Figs. 8 and 10), and terminate with a negative excursion.

In the Shublik Mountains, $\delta^{13}C$ profiles through the lower Nanook Limestone begin with a positive excursion followed by a smooth negative anomaly, from +2‰ to −5‰ and back to +2‰. This negative anomaly is developed in the ichnogenera-bearing turbidites. In the Sadlerochit Mountains, the anomaly is basally truncated as the lower Nanook Limestone onlaps from the south. In both ranges, $\delta^{13}C$ values oscillate around +1‰ for the bulk of unit N1, drop to negative values for ~100 m, and then return to positive values in the limestones of unit N2.

Oxygen-isotope profiles are smooth and heavy in the Katakturuk Dolomite relative to other Neoproterozoic $\delta^{18}O$ profiles (Jacobsen and Kaufman, 1999), particularly through K3 and K4 (Fig. 10). Negative excursions commonly exist in the few meters below exposure surfaces at the major disconformities and are likely due to alteration from meteoric water. In units K1–K3, values are scattered between 0‰ to −5‰ with no obvious trends (see supplementary data [footnote 1]). In K3, values hover around −1‰, and in K4, values decline smoothly from +1‰ to −5‰. Oxygen isotopes in limestone beds are uniformly lower and are perhaps more susceptible to alteration. This can be seen most clearly at the abrupt negative shift in values at the major limestone-dolostone transition within the upper Nanook Limestone (Fig. 10).

Detrital Zircon Geochronology

Sample Selection and Analytical Methods

Three 2–5 kg samples were collected from clastic rocks stratigraphically beneath the Katakturuk Dolomite for detrital zircon geochronology. Two samples (samples 95-14 and 95-15) were collected from unit O.G. at localities ~8 km east of Nularvik Creek (Fig. 4B). The third sample (sample F608) is from the top of the Hula Hula diamictite exposed along Nularvik Creek (Fig. 4B). Sample 95-14 was taken from a 5- to 10-cm-bedded, coarse-grained sandstone interlayered with finer-grained sandstone and siltstone. Sample 95-15 was collected from a 5-m-thick fine-grained quartz arenite layer. F608 was sampled from an unsorted diamictite composed of angular to subangular gravel and pebble clasts of quartzite and basalt in a bimodal matrix of silt and grit.

Zircons from each of the three samples were separated by standard crushing and gravimetric techniques and subpopulations for analysis, were randomly selected. Detrital zircons from samples 95-14 and 95-15 were analyzed by both the TIMS (thermal ionization mass spectrometry) and LA-ICP-MS (laser ablation–inductively coupled plasma–mass spectrometry) methods. Grains from sample F608 were analyzed by the LA-ICPMS method only. The data are presented in Tables DR2 and DR3 (supplementary data; see footnote 1). Discussion of the results below is largely based on LA-ICPMS analyses that are no more than 10% discordant. The $^{206}Pb/^{238}U$ ages are used for interpretation of grains <1.0 Ga, whereas the $^{207}Pb/^{206}Pb$ age is used for grains >1.0 Ga.

Representative grains from unit O.G. were analyzed as single grains by the TIMS method at the University of California, Santa Barbara. After random selection, 20 grains from each of samples 95-14 and 95-15 were abraded to ~75% of their original size. Analytical procedures and data reduction followed that outlined in McClelland and Mattinson (1996). Plotting of Tera-Wasserburg and probability density plots utilized the program of Ludwig (2003). Results of this initial phase of the study were discussed in McClelland (1997).

Additional zircon grains from unit O.G. and zircon grains from the Hula Hula diamictite (sample F608) were analyzed for U-Pb using a New Wave UP-213 (213 nm, Nd:YAG) laser system coupled to a ThermoFinnigan Element 2 ICP-MS instrument housed at Washington State University. Analysis and data reduction followed procedures outlined in Chang et al. (2006). The laser operated with a fluence of 10–11 J/cm^2 and a frequency of 10 Hz, with an ablation spot ~30 µm in diameter and 25 µm deep. Signals were collected for 36 seconds in 300 sweeps with a counting efficiency of 86% per analysis. A blank was measured before each analysis, and a set of known standards was measured every 5–10 analyses for correction of U and Pb elemental fractionation mass bias in the mass spectrometer. Standards used to monitor fractionation were the 564 Ma Peixe (Gehrels, 2006, personal commun.), the 1099 Ma FC-1 (Paces and Miller, 1993), and the 419 Ma R33 (Black et al., 2004). Standards R33 and FC-1 were used to evaluate fractionation corrections based on Peixe.

Results

All three samples yielded diverse populations of round to elongate, clear to red-colored, and well-rounded grains. Most grains have fine oscillatory zoning revealed in cathodoluminescence (CL) images that is typical of igneous zircon. Zoning is commonly truncated at grain margins. Approximately 10%–15% of the grains appear to have core-rim relationships based on variation in CL properties. The presence of xenocrystic components and Pb-loss in some grains is established by the observed discordance of some analyses. Data

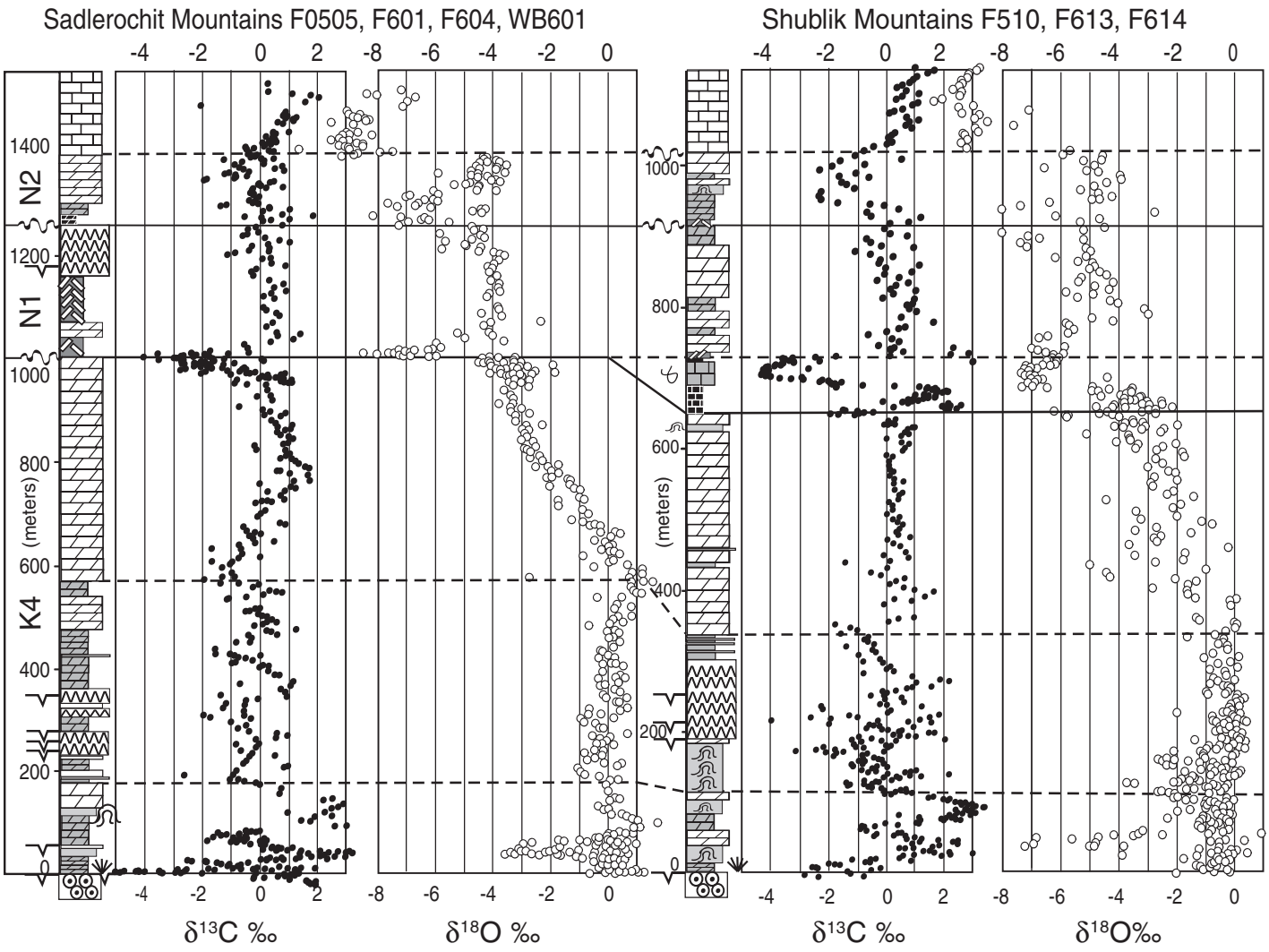

Figure 10. Carbon- and oxygen-isotope chemostratigraphy of map units K3, K4, N1, and N2 in the Sadlerochit and Shublik Mountains. Legend for symbols is the same as Figure 7.

from grains that gave complex age spectra during LA-ICPMS analysis are not reported since they clearly represent mixture of multiple age domains.

Ages from the three samples overlap in range from 760 ± 11 to 3420 ± 11 Ma but vary in relative abundance (Figs. 11A–11C). Peaks are observed in all samples at ca. 1380, 1465, 1880, 1980, 2025, 2065, 2680, and 2735 Ma. In contrast to samples from unit O.G., the diamictite sample also contains a significant number of grains ranging from 1.0 to 1.2 Ga. Neoproterozoic grains are present in all samples as well, with several ages between 850 and 890 Ma. The youngest concordant analyses were observed in sample 95-15, which contained grains with $^{206}Pb/^{238}U$ ages of 760 ± 11 and 763 ± 13 Ma (Fig. 11D). These two analyses limit the depositional age of the unit O.G. clastic sequence to be younger than ca 760 Ma.

DISCUSSION

The Fidelity of Chemostratigraphic Signals

The $\delta^{13}C$ composition of carbonate rocks is relatively immune to pervasive diagenetic changes because pore fluids are buffered by a large rock reservoir (Veizer et al., 1999). Carbon-isotope profiles through the Katakturuk Dolomite are consistent and reproducible in multiple sections, further indicating that large-scale diagenesis is unlikely. Moreover, particularly in units K4 and N1, $\delta^{18}O$ values are remarkably heavy and smooth except over obvious exposure surfaces that have demonstrably experienced meteoric alteration. Carbon-oxygen cross-plots illustrate that several of the isotopic excursions do not covary in both isotopic systems (see supplementary data, Fig. DR1 [footnote 1]), indicating that these excursions cannot be explained simply with alteration.

Despite significant heterogeneity in the $\delta^{13}C$ of the modern ocean (Kroopnick, 1985), large secular changes in $\delta^{13}C$ at individual sites can be correlated globally (Veizer et al., 1999; Saltzman et al., 2000). This is due to the long residence time of carbon, which is ~150 times the mixing time of the ocean (Kump and Arthur, 1999). This ratio was likely even larger in the Neoproterozoic, when higher concentrations of atmospheric CO_2 were needed to compensate for a faint young sun (Walker et al., 1981). Swart and Eberli (2005) demonstrated that $\delta^{13}C$

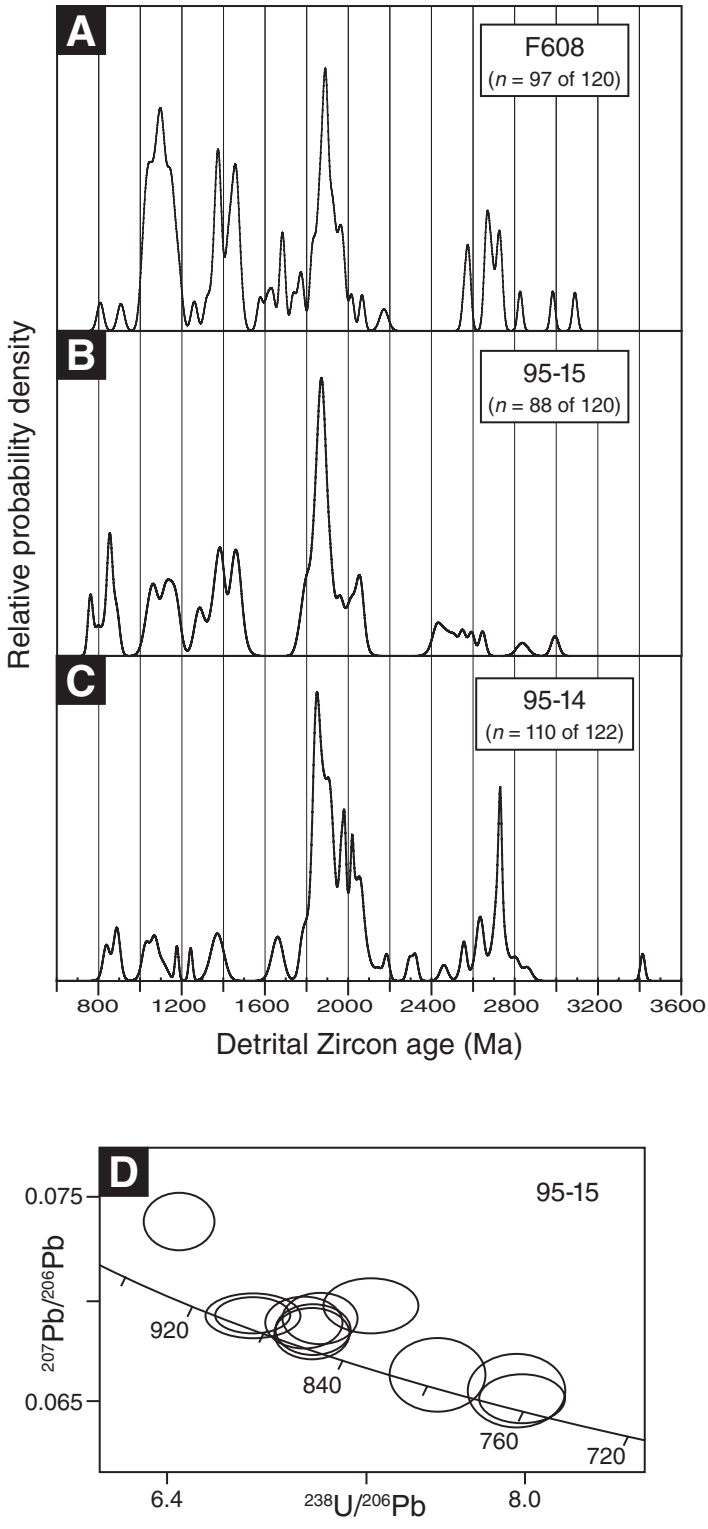

Figure 11. (A–C) Probability density plots of detrital zircon ages for (A) sample F608, (B) sample 95-15, and (C) sample 95-14. For ages >1.0 Ga, the ^{204}Pb-corrected ^{207}Pb/^{206}Pb ages are used, whereas for ages <1.0 Ga, the ^{207}Pb-corrected ^{206}Pb/^{238}U ages are used for plotting. (D) Tera-Wasserburg plot of the youngest Neoproterozoic detrital zircons from sample 95-15. Error ellipses are plotted from data uncorrected for common Pb at the 1σ uncertainty level.

values of Miocene-Pleistocene periplatform carbonates on the Great Bahaman Bank only vaguely follow the δ^{13}C of pelagic sediments, yet conclude that the δ^{13}C values can be correlated between different sites. Thus, although using the δ^{13}C values of platformal carbonates to quantify global changes in the carbon cycle may be compromised by complications in the carbon source and early diagenesis, carbon-isotope chemostratigraphy remains a useful correlation tool. Moreover, the Bahaman study (Swart and Eberli, 2005) emphasizes the necessity of linking sequence stratigraphy and chemostratigraphy to assess the likelihood of diagenetic effects associated with sea-level change.

In the Katakturuk Dolomite, upper- and mid-ramp facies are composed of light-colored, organic-poor dolomite. Limestone is present exclusively in lower-slope rhythmites, turbidites, and in the cryptic-microbialite structures that overlie the Hula Hula diamictite. The general pattern of dolomites dominating shallow water settings and limestones present only in deeper water settings is a feature of many late Neoproterozoic successions globally (e.g., Knoll and Swett, 1990; Pelechaty, 1998). While evidence for primary aragonite precipitation is present in the upper half of unit K2 and at the base of K4 in the form of pseudomorphosed crystal fans, early or primary dolomitization is suggested by the retention of original sedimentary textures, and the uniformity of the dolomitization. Furthermore, cements have δ^{13}C and δ^{18}O values comparable to that of the host carbonate (see supplementary data tables [footnote 1]). The low susceptibility of dolostones to meteoric corrosion, and low relative permeability, as pore-spaces in grainstones and ooids are commonly filled with dolomite cements, may have been important in isolating the dolostones during burial diagenesis. Meanwhile, the few interbedded limestones have very depleted oxygen-isotope values and are commonly tightly folded. Perhaps the early or primary dolomitization coupled with early cementation on the platform "locked in" oxygen-isotope values, preventing isotopic equilibrium with pore fluids during later burial and recrystallization.

As diagenetic recrystallization can completely replace the original population of oxygen atoms in the rock, δ^{18}O trends in ancient carbonates are typically used to assess alteration and ignored as a seawater proxy (Brand and Veizer, 1981; Banner and Hanson, 1990). Nonetheless, the smooth trend of the oxygen-isotope profile of units K4 and N1, and the reproducibility in sections that were deposited over 10 km apart, suggests a primary signal. On multi–million-year time scales, the oxygen-isotope composition of seawater is controlled by the exchange of oxygen with sili-

cate rocks (Muehlenbachs and Clayton, 1976; Walker and Lohmann, 1989; Muehlenbachs, 1998). For typical water-rock interaction rates, the maximum change in the oxygen-isotope composition of seawater is ~1‰ per 100 million years (Walker and Lohmann, 1989). Thus, the trend in the $\delta^{18}O$ record from the Katakturuk Dolomite cannot reflect the evolution of the oxygen-isotope composition of seawater due to hydrothermal exchange.

The –4‰ $\delta^{18}O$ shift in unit K4 is similar in magnitude, but in the opposite direction, to the deep-sea $\delta^{18}O$ trend of benthic forams from the Paleocene-Eocene Thermal Maximum to the Quaternary glacial periods (Zachos et al., 2001). Roughly half of the Cenozoic enrichment is due to the temperature-dependent fractionation of calcite with seawater, and half to the temporary sequestration of isotopically light oxygen in continental ice sheets (Zachos et al., 2001). Although there is evidence in Newfoundland for the presence of regional ice sheets at ca. 582 Ma (Anderson and King, 1981; Bowring et al., 2003), no well-dated glacial deposits have been identified in the latest Ediacaran or Early Cambrian. Thus, we are left with temperature and salinity to explain the –4‰ shift. In an ice-free ocean, a 4‰ decline in $\delta^{18}O$ corresponds to ~16° of warming (O'Neil et al., 1969). Although the mechanism for such a large change in surface ocean temperature is not readily apparent, a similar $\delta^{18}O$ trend has been reported in late Ediacaran successions in Oman (Burns and Matter, 1993) and China (Zhou and Xiao, 2007).

Lithologically, the inflection in the $\delta^{18}O$ record corresponds with a transition from strata dominated by microbialaminites to strata dominated by crossbedded grainstones. The former were deposited in an intertidal to supratidal setting, whereas the latter likely formed as sand bars in a high-energy environment. Our carbon-isotope correlations also indicate that this transition roughly corresponds to a significant increase in sedimentation rate (see below). A corresponding change in basin dynamics could have tapped a new source of water with a different, perhaps more meteoric composition. An increase in accumulation rate coupled with the higher primary porosity and permeability of grainstones could have also led to a progressive increase in the depth of cementation.

Intrabasinal Correlations and Reconstruction of a Carbonate Platform Margin

Stromatolite elongation is a product of wave scour from a predominant direction. Elongation tends to be normal to the shoreline due to wave refraction, analogous to "spur-and-grove" structures of modern reefs (Goldring, 1938; Hoffman, 1967). However, like crossbeds in grainstones, interpretation of this feature can be complicated locally by longshore ebb-tide currents. Columnar, laterally linked stromatolites near the base of unit K4 are predominantly oriented N-S, presumably normal to shoreline (Clough and Goldhammer, 2000). Higher in K4, bulbous stromatolites yield more variable orientation measurements. No systematic facies changes are apparent E-W, along the ranges, within the Katakturuk Dolomite.

Reconnaissance carbon-isotope analyses through the black limestones of the Fourth Range give values averaging ~+9‰ (supplementary data tables [footnote 1]). Such enriched $\delta^{13}C$ values are rare in Phanerozoic strata, present only in transient excursions (Saltzman, 2005), but have been documented in the Neoproterozoic strata of Mongolia (Brasier et al., 1996) and Canada (Hoffman and Schrag, 2002). We suggest that the limestones in the Fourth Range are an expanded deep-water equivalent of unit K1; however, as neither the top nor the bottom of the sequence is exposed in the Fourth Range, this correlation lacks discrete tie lines, and particular isotopic features cannot be compared.

The basal truncation of the unit K1 in the Shublik Mountains (Fig. 3) is a stratigraphic puzzle. Although the basal contact of K1 in not exposed, map relations indicate that the contact is parallel to bedding and the amount of K1 above the contact is consistent throughout the range (Fig. 4C). Structurally, it is not apparent how the lower portion of K1 could be faulted out. Thus, the simplest interpretation is that the contact is depositional and that ~400 m of the Katakturuk Dolomite is missing from the Shublik Mountains on a paleo-high. If the Mount Copleston volcanics delineate a rifting event, as suggested by Clough and Goldhammer (2000), then this paleo-high may have developed with block rotation above a listric normal fault. Moreover, this paleo-high may have the source of the volcaniclastics at Kikitak Mountain, and the nucleus for a rim on the platform margin.

In contrast to Clough and Goldhammer (2000), who argued for a SW-deepening ramp geometry persisting throughout the Katakturuk Dolomite, we suggest that the platform transformed multiple times from a rimmed-margin to a south-facing ramp in response to base level change. In particular, in the aftermath of a major transgression and progradation, a ramp geometry developed, whereas during relative shallowing and aggradation a flat-topped, rimmed-margin developed, as is seen in the Pliocene-Quaternary evolution of the Great Bahaman Bank (Eberli and Ginsburg, 1989). Our chemostratigraphic and lithostratigraphic correlations, combined with facies patterns, indicate that most of unit K1 in the Sadlerochit Mountains was deposited in a back reef environment, while the lower ~300 m of K1 at Kikitak Mountain was deposited on the outer slope (Fig. 3). As the margin prograded, shelf-edge deposits reached the Kikitak Mountain sections, with a ramp possibly developing in the upper portion of K1. Before the deposition of K2, base level fall exposed the margin, and rim or flat-top profile formed, creating a geometry favorable for the restricted lagoonal environment indicated by the large crystal fans and exposure surfaces in the upper portion of K2 in the Sadlerochit Mountains. With the major transgression at the base of K3, south-facing ramp geometry developed and persisted to the calcretized pisolite at the top of K3. Back reef deposits are also present in the lower portion of K4, indicating renewed development of a rimmed shelf, but again, with progradation, it is likely that a ramp formed in the upper portion of K4.

Clough and Goldhammer (2000) suggested that the Katakturuk Dolomite was much thinner in the Shublik Mountains due to truncation under the sub-Nanook unconformity. Instead, our mapping and chemostratigraphy suggests that the Katakturuk is thinner in the Shublik Mountains because of facies changes and a basal truncation (Figs. 3 and 4C). Moreover, our redefinition of units in the Sadlerochit Mountains, which is supported by carbon and oxygen-isotope chemostratigraphy (Fig. 10), suggests that very little, if any, of unit K4 is missing from the Shublik Mountains. By including unit N1 with the Katakturuk Dolomite, Robinson et al. (1989) inferred that the upper ~300 m of the Katakturuk Dolomite is missing in the Shublik Mountains under an unconformity, while the lower Nanook Limestone is absent in the Sadlerochit Mountains. Our new correlations eliminate this problem of missing strata and suggest that the carbonate-shale turbidites and rhythmites at the base of the lower Nanook Limestone were deposited during a northward migrating onlap (present coordinates).

Global Correlations

Although the nomenclature for a pre-Ediacaran period has yet to be formally defined, to avoid the problematic terms "Sturtian" and "Marinoan," we herein informally use "Cryogenian" to refer to the time period beginning with the oldest Neoproterozoic glacial deposits and ending with the ca. 635 Ma end-Cryogenian glacial deposits. Carbon-isotope composite curves from strata bracketing Neoproterozoic diamictites broadly suggests two pre-Ediacaran glacial episodes globally (Halverson et al., 2005), one during the early-Cryogenian ending at 713.5

± 2 Ma (Bowring et al., 2007), and a second end-Cryogenian glaciation ending between 635.51 ± 0.54 Ma and 635.23 ± 0.57 Ma (Condon et al., 2005).

Hula Hula Diamictite

A glacial origin of the Hula Hula diamictite is suggested by the presence of cobble- to boulder-sized foreign clasts in a fine, laminated matrix. These clasts are bed penetrating and truncating (Fig. 6A), and as such are interpreted as ice-rafted debris. An early Cryogenian age of the Hula Hula diamictite is inferred from the chemostratigraphy of the overlying Katakturuk Dolomite.

Unit K1

The dark-colored limestone at the base of unit K1 contains cryptic-microbial "roll up" structures that are also present in the early–Cryogenian Rasthof cap carbonate of Northern Namibia (Hoffman et al., 1998a). As these microbial structures are otherwise in deep-water, rhythmite facies, it is possible that these were formed by nonphotosynthetic organisms. In the Sadlerochit Mountains, within the basal 20 m of K1, $\delta^{13}C$ values rise from –2‰ to +4‰. This $\delta^{13}C$ profile is also comparable to that of the Rasthof Formation (Yoshioka et al., 2003). Higher in K1, the enriched $\delta^{13}C$ values and the positive, concave-upward profile are typically seen in strata deposited during the Cryogenian interglacial period (Halverson et al., 2005), In the uppermost parasequence of K1, $\delta^{13}C$ values drop to 0‰ but are scattered. Although less negative, this drop is likely correlative to the beginning of the Trezona anomaly (McKirdy et al., 2001; Halverson et al., 2002), which may have been largely removed under the sub-K2 disconformity.

The Nularvik Cap Carbonate, Unit K2

Although no glacial diamictites have been identified, unit K2 contains sedimentary textures in a particular order that are characteristic of basal Ediacaran cap carbonates globally (Allen and Hoffman, 2005; Hoffman et al., 2007). The basal portion of K2 (the "cap dolomite" *sensu* Hoffman et al., 2007) has an average thickness of 35 m, and is composed primarily of a buff-colored, hummocky, fine, laminated, micropeloidal dolomite with low-angle cross stratification, as is the case in Australia (Kennedy, 1996), the Mackenzie Mountains (Aitken, 1991; James et al., 2001), Namibia (Allen and Hoffman, 2005), and elsewhere. Tubestone stromatolites are present in the Nularvik cap carbonate and have previously been documented in basal Ediacaran cap carbonates in Namibia (Hoffman et al., 1998a), Death Valley (Wright et al., 1978), and the Mackenzie Mountains (James et al., 2001). Unit K2 also contains giant wave ripples, which have been documented in several basal Ediacaran cap dolostones globally (Allen and Hoffman, 2005). Unlike crystal fans that are associated with basal Ediacaran cap carbonates elsewhere (Aitken, 1981; Peryt et al., 1990; Soffer, 1998; James et al., 1999), the crystal fans in unit K2 are developed in a shoal complex rather than transgressive ribbonite facies, and contain multiple exposure surfaces and isotopic discontinuities. Occasionally, individual fans are tipped over on their side from the buckling of teepees. Together these sedimentary features suggest a restricted, back reef setting.

The lack of glacial deposits under unit K2 can be attributed to poor preservation potential as the glacio-eustatic sea-level drop left the carbonate platform exposed until the postglacial transgression. Glacial diamictites are also rare under the Keilberg cap carbonate on the Otavi platform in Northern Namibia (Hoffman et al., 1998b).

Carbon-isotope profiles of unit K2 display a sigmoidal shape with a nadir at –2‰ (Fig. 7). Normalized to the thickness of the cap dolostone, this pattern is similar to the basal Doushantuo cap carbonate in South China (Jiang et al., 2003; Zhou and Xiao, 2007), which has been dated at 635.23 ± 0.57 Ma (Condon et al., 2005). The carbon-isotope profile of cap dolostone of unit K2 is also reminiscent of that seen in slope sections of the Maieberg cap carbonate in northern Namibia, where shelf sections are 3‰–4‰ lighter than foreslope sections (Hoffman et al., 2007). Rather than an isotopic gradient, Hoffman et al. (2007) suggested that the slope sections were deposited diachronously during the post-glacial transgression. In this model, the relatively enriched values of the Nularvik cap carbonate would imply that it was deposited relatively early compared to shelf sections in Namibia, and then unit K2 was truncated by exposure surfaces and debris flows before seawater reached extremely negative values.

Carbon-isotope values are highly variable through the crystal-fan–dominated portion of unit K1. This is perhaps due to restriction and exposure. Isotopic scatter, evidence of exposure, and pervasive cementing is also a common feature in the upper portion of many Doushantuo cap dolostone sections in China (Jiang et al., 2003) and Jbeliat cap dolostone sections in Mauritania (Hoffman and Schrag, 2002; Shields et al., 2007). We suggest that during the end-Cryogenian glaciation and resultant sea-level fall, a flat-topped shelf developed. During the post-glacial transgression the shelf flooded and then became, restricted, leading to enriched and scattered isotopic values. Eventually, as the transgression progressed, there was major slope failure, and the margin returned to a ramp geometry. This slope failure, as demonstrated by multiple debris flows in the lower part of K3 (Fig. 7), accounts for the absence of early Ediacaran strata between units K2 and K3 (from ca. 630 to 615 Ma; Fig. 12).

Unit K3

The $\delta^{13}C$ profile through unit K3 is similar to the early Ediacaran carbon-isotope values from the Khufai Formation of Oman (Fig. 12; Burns and Matter, 1993). At the top of unit K3, $\delta^{13}C$ values decrease to 0‰ where strata are truncated under the base of the K4 karstic surface (Fig. 8). Negative values in the pisolite may be due to alteration and should not be used for correlation (see supplementary data, Fig. DR1 [footnote 1]). We interpret this surface, which contains vadose pisoids, as a major exposure surface coeval with the sea-level fall associated with the regional ca. 582 Ma Gaskiers glaciation (Bowring et al., 2003).

Unit K4

Aragonite crystal fans in the basal 10 m of unit K4 are similar in size to those described in the Johnny Formation of Death Valley (Pruss and Corsetti, 2002). From the depleted values in these strata, $\delta^{13}C$ values rise to two positive anomalies before oscillating around zero (Fig. 10). The upper ~300 m of K4 is characterized by positive stable $\delta^{13}C$ plateau with values ranging from 0‰ to +2‰ before the large negative anomaly at the K4-N1 transition. This negative trend is similar to terminal Ediacaran profiles through the Egan and Boonall Formations in northwestern Australia (Corkeron, 2007), the Nama Group of southern Namibia (Saylor et al., 1998), the Turkut Formation of northeast Siberia (Pelechaty et al., 1996), the Buah and Ara Formations of Oman (Burns and Matter, 1993; Amthor et al., 2003), and the Denying Formation of South China (Zhou and Xiao, 2007). Although this isotopic interval has been termed the "+2‰ plateau" in Namibia (Saylor et al., 1998), values closer to 0‰ are present in Siberia (Pelechaty et al., 1996). In Oman, stable values near 0‰ have not been documented in the Ediacaran until after the Shuram anomaly (Burns and Matter, 1993; Amthor et al., 2003). Although late Ediacaran fossils have not been identified in unit K4, this may be due to the lack of proper facies, and heavy recrystallization, the latter possibly obfuscating calcifying metazoans.

The Nanook Limestone

The two-pronged $\delta^{13}C$ anomaly in the basal Nanook Limestone is reminiscent of the Precambrian-Cambrian boundary anomaly in Oman (Amthor et al., 2003), Morocco (Maloof

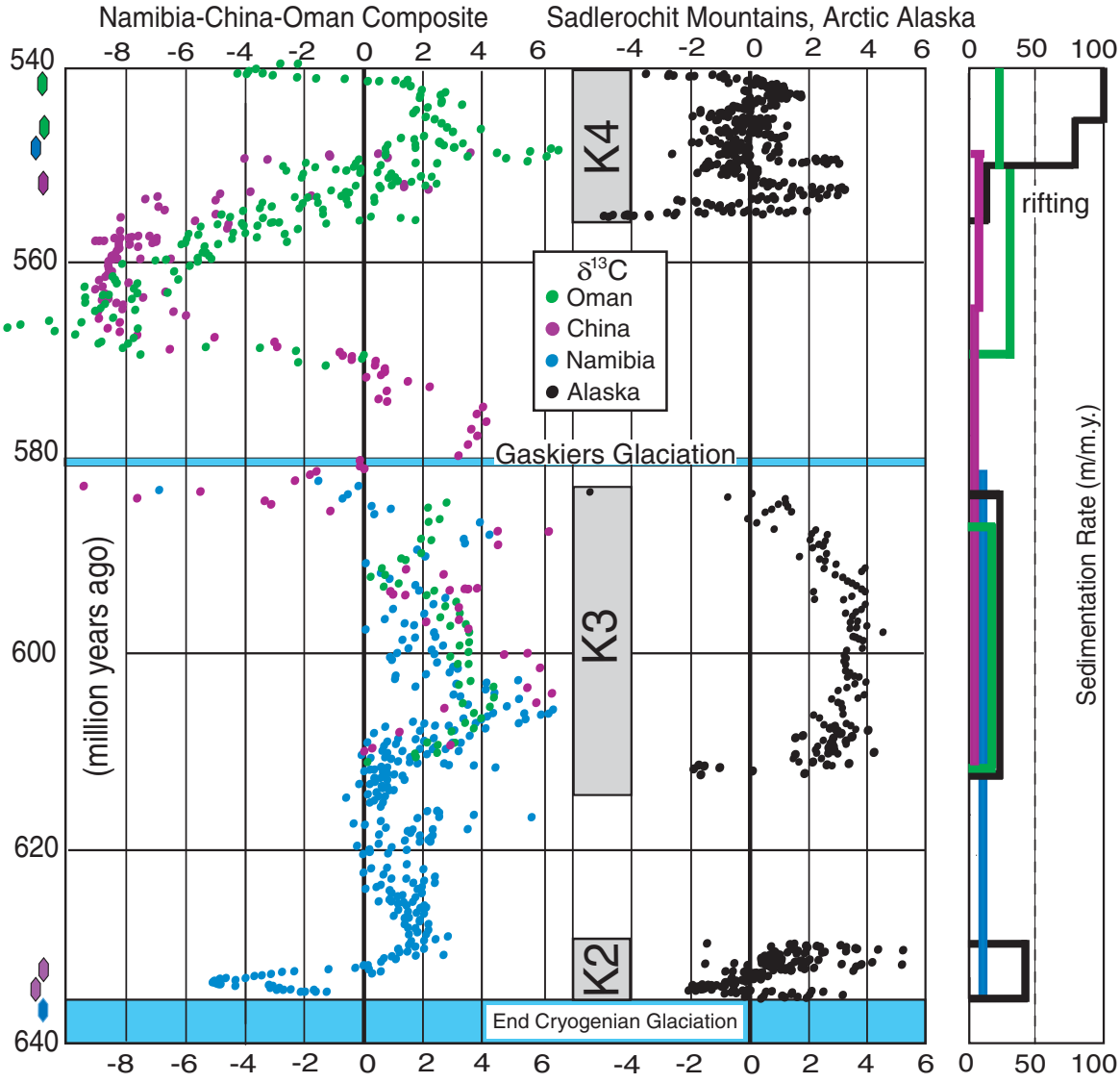

Figure 12. Composite Ediacaran $\delta^{13}C$ curve. Namibian data (blue dots) are from the Tsumeb and Elandshoek Formations (Halverson et al., 2005). Oman data (green dots) are from the Khufai, Shuram, and Ara Formations (Amthor et al., 2003; Cozzi et al., 2004; Fike et al., 2006). China data (purple dots) are from the Doshantuo Formation (McFadden et al., 2008). Alaska data (black dots) are from sections F501, F502, F505, F601, F602, F603, and F605, all in the Sadlerochit Mountains. Color codes hexagons are thermal ionization mass spectrometer (TIMS) U/Pb zircon dates on ash beds from Namibia (Grotzinger et al., 1995; Hoffmann et al., 2004), Oman (Bowring et al., 2008), and South China (Condon et al., 2005). Sedimentation rates are averaged over the interval which unconformably bound sequence is stretched. See supplementary data, Figure DR2 [footnote 1] for a discussion of the construction of the curve.

et al., 2005), Siberia (Kaufman et al., 1996), and elsewhere. However, this correlation would require that the lower Nanook Limestone was deposited by ca. 535 Ma, prior to the pronounced positive $\delta^{13}C$ anomalies in the Nemakit-Daldyn (Maloof et al., 2005; Kouchinsky et al., 2007), with the fossiliferous upper Nanook Limestone deposited in the Late Cambrian and Ordovician. Alternatively, the $\delta^{13}C$ anomaly in the Lower Nanook can be correlated with the Botomian-Toyonian boundary anomaly as documented in the Sekwi Formation of the northwestern Cordillera (Dilliard et al., 2007), with much of the Early Cambrian missing under the K4-N1 contact. While the ichnogenera suggest a Cambrian or younger age, unfortunately they do not provide more resolution (Soren Jensen, 2008, personal commun.), and chemostratigraphic correlations of the lower Nanook Limestone remain ambiguous.

Basin Dynamics

The ca. 760 Ma detrital zircons in the underlying unit O.G. provide a maximum age constraint for the deposition of the Katakturuk Dolomite. If we assume that the Hula Hula diamictite is an early-Cryogenian glacial deposit, we are provided with additional age constraints. A maximum age of the early-Cryogenian glaciation is provided by a U/Pb TIMS date of 726

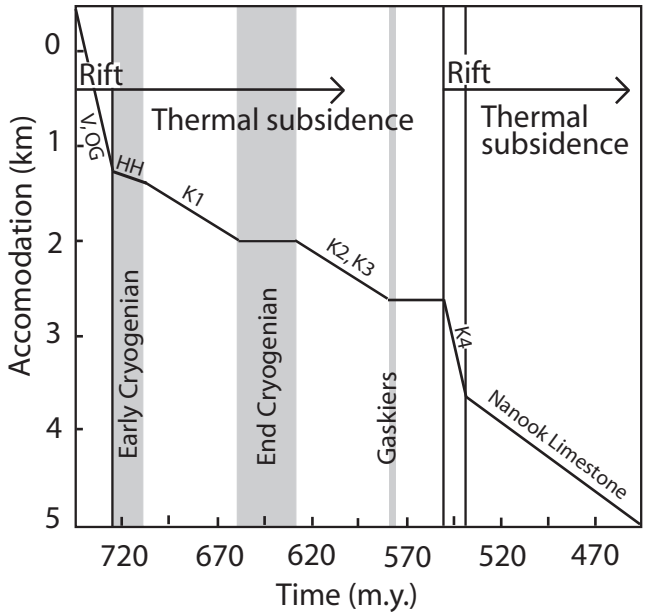

Figure 13. Simple basin model for deposition of the pre-Devonian strata in the northeastern Brooks Range. Cumulative thickness of unit O.G. and the Mount Copleston volcanics (OG, V) is uncertain but approximated to be over 1 km with deposition beginning sometime after 760 Ma but before 726 Ma, based on the model that these are riftogenic deposits. The thickness for the Hula Hula diamictite (HH) is taken from the Kikitak Mountain area. Thicknesses for the Katakturuk Dolomite are from the Sadlerochit Mountains. No correction for compaction is used because the succession is composed predominantly of dolomite. Age constraints for deposition are based on correlation with the early- and end-Cryogenian glaciations and with the Ediacaran composite $\delta^{13}C$ curve (Fig. 12). Thickness of the Cambrian–Late Ordovician Nanook Limestone is from the Shublik Mountains. See supplementary data [footnote 1] for the range of thicknesses of the units.

± 2 Ma Leger granite in Oman (Bowring et al., 2007), which underlies the Ghubrah diamictite. Older ages have been reported from the Pocatello Group in Idaho (Fanning and Link, 2004) and from the Gariep Belt in Namibia (Frimmel et al., 1996), but the stratigraphic relationship between these ages and the glacial deposits is less certain. The Ghubrah diamictite also contains volcanic zircons with a U/Pb TIMS age of 713.5 ± 2 Ma (Bowring et al., 2007), perhaps dating the deglaciation. In our subsidence model (Fig. 13), we use this age as a best guess for the onset of deposition of the Katakturuk Dolomite. A maximum age of the duration between the early- and end-Cryogenian glaciations is provided by a U-Pb sensitive high-resolution ion microprobe (SHRIMP) age of 663 ± 4 Ma from the Datangpo Formation of South China (Zhou et al., 2004). Taking these age constraints, we are left with a maximum accumulation rate of K1 in the Sadlerochit Mountains of 10.6 m/m.y. (530 m in 50 m.y.).

In the aftermath of the ca. 635 Ma end-Cryogenian glaciation, regions of active subsidence accommodated huge thicknesses of basal Ediacaran strata (Halverson et al., 2002). However, unit K2 contains multiple exposure surfaces, and some of the middle Ediacaran is likely missing from the Katakturuk Dolomite, again suggesting weak subsidence. Carbon-isotope correlations with Namibia and Oman (Fig. 12) suggest that units K2 and K3 were deposited between ca. 635 Ma and 582 Ma. As the thickest continuous section of K2 and K3 in the Sadlerochit Mountains measured 563 m, our calculated accumulation rate for K2 and K3 is again at 10.6 m/m.y. These slow accumulation rates indicate that units K1–K3 were deposited on a thermally subsiding passive margin with no active stretching (Fig. 13).

Carbon-isotope correlations of unit K4 with the global $\delta^{13}C$ curve for the latest Ediacaran suggest a marked increase in sedimentation rate (Fig. 12). A late Ediacaran rift along the southern margin of the North Slope subterrane is indicated not only by the increase in sedimentation rate, but also by two low-angle unconformities in the overlying Cambrian strata. An additional subsidence mechanism after Cryogenian rifting is needed to accommodate the 1300–1000 m Cambrian–Late Ordovician carbonate strata in the Shublik Mountains. Moreover, immediately south of Kikitak Mountain in the Romanzof Mountains, the laterally equivalent Neruokpuk Schist and overlying Cambrian strata are over 5 km thick (Reiser et al., 1980). These deposits can be accounted for with rifting along a growth fault. Lastly, Cambrian volcanic rocks in the Romanzof Mountains have ocean-island basalt chemical affinities (Moore, 1987), and farther south, the Doonerak fenster contains Paleozoic volcanic and sedimentary rocks that have been interpreted as the remnants of a volcanic arc (Julian and Oldow, 1998), both suggesting the development of Paleozoic oceanic crust on the southern margin of the North Slope subterrane.

Paleogeography and the Origin of the Arctic Alaska–Chukotka Microplate

Although paleomagnetic constraints on the Arctic Alaska–Chukotka microplate are lacking, paleogeographic reconstructions can be assessed through stratigraphic and biogeographical connections. Early Paleozoic conodonts in the Arctic Alaska–Chukotka microplate and the Farewell and Alexander terranes all have a mixed affinity, containing many forms that are otherwise exclusive to Siberia, and others that are exclusive to Laurentia (Dumoulin et al., 2002). In the Shublik Mountains, the Nanook Limestone contains the pentamerid brachiopod *Tcherskidium*, which is characteristic of peri-Siberian terranes (particularly the Kolyma Region and Kazakhstan), such as the Farewell terrane (Blodgett et al., 2002).

The detrital zircon results from unit O.G. and the Hula Hula diamictite contain several grains ranging from ca. 760 to 890 Ma. These ages are similar to basement ages observed in the Farewell terrane (Bradley et al., 2006). The range and abundance of Mesoproterozoic ages are consistent with those observed in the Farewell terrane as well (Bradley et al., 2007).

Although a Neoproterozoic to Paleozoic carbonate platform has been described on the Hammond subterrane (Dumoulin et al., 1998), these strata are separated from the carbonates of the Shublik and Sadlerochit Mountains by deep-water deposits in the Romanzof Mountains, the Endicott terrane, and a fragment of a putative island arc on the Doonerak fenster (Fig. 1). The Hammond subterrane is separated from the Farewell terrane by the arc volcanics of the Angayucham subterrane. While all of the subterranes in the Arctic Alaska–Chukotka microplate and the Farewell terrane have mixed Laurentian and Siberian fauna,

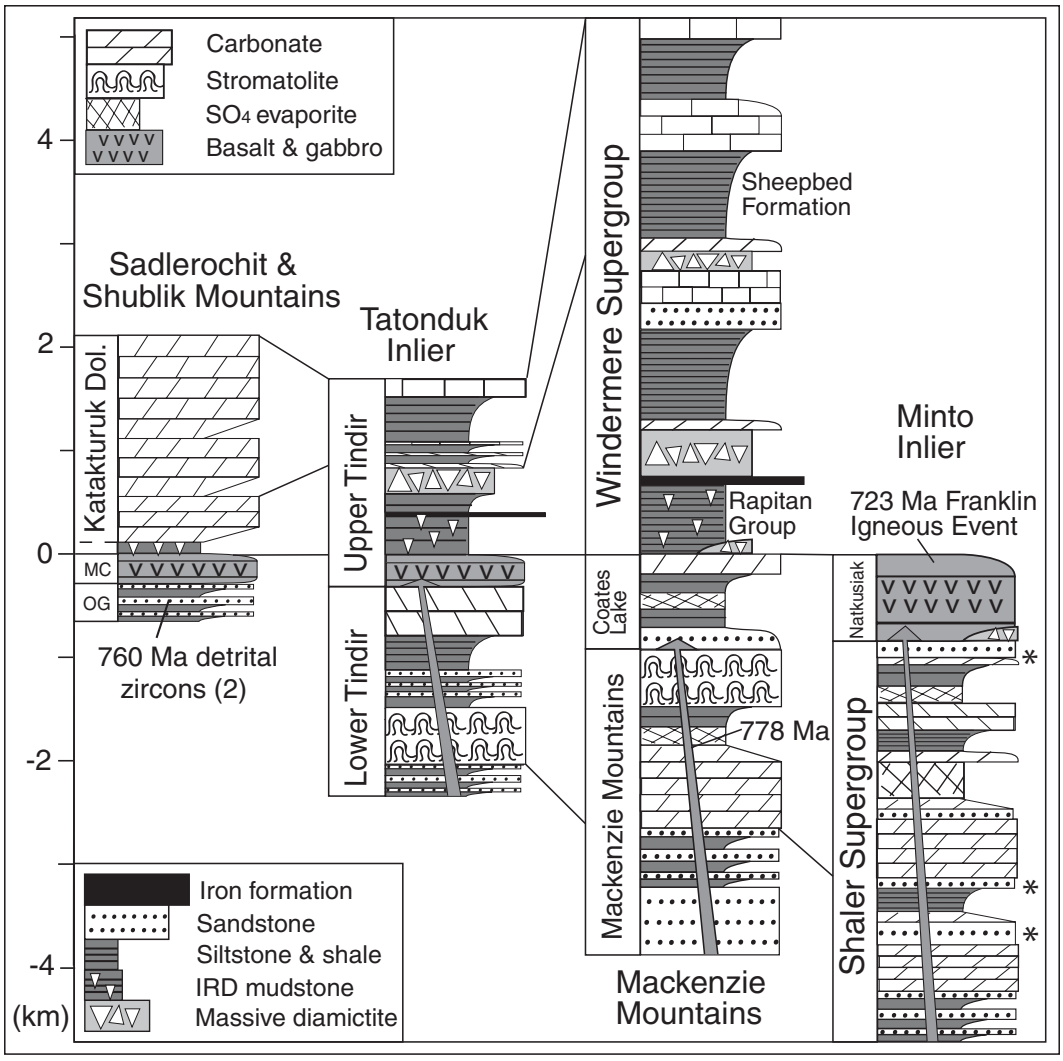

Figure 14. Stratigraphy of Neoproterozoic strata in the Northwestern Cordillera, from left to right: the Mackenzie Mountains (Halverson et al., 2007a); the Tatonduk Inlier (personal observations); Minto Inlier from Victoria Island (Young, 1981); the Shublik and Sadlerochit Mountains, this work. "MC" designates the Mount Copleston volcanics. Asterisks alongside the Shaler Supergroup mark the stratigraphic position's detrital zircons sampled by Rainbird et al. (1992). IRD mudstone is a fine-grained, laminated diamictite containing dropstones that are interpreted as ice-rafted debris. Sections are tied to the base of the glacial deposits in the Rapitan Group.

and geologically have more in common with each other than either Siberia or Laurentia, the geometry of their Neoproterozoic and Paleozoic juxtaposition is unclear.

It is not obvious what rifted away from the North Slope subterrane in the Late Ediacaran to initiate subsidence. Potential candidates include the rest of the Arctic Alaska–Chukotka microplate, other peri-Siberian terranes, Laurentia, and Siberia. Zonenshain et al. (1990) suggested that the Arctic Alaska–Chukotka microplate is part of an Arctic continent, Arctidia, which is partially submerged under the Arctic Ocean in the form of the East Siberian Shelf and the Chukchi Borderland. In this scenario, Arctidia consists of attenuated continental crust that has been stretched multiple times forming opposing margins on the North Slope subterrane and the rest of the Arctic Alaska–Chukotka microplate.

The Franklin dikes of northwestern Laurentia, which have been dated with U-Pb at 723+4/−2 Ma (Heaman et al., 1992), and their extrusive expression, the Natkusiak Formation flood basalt, are potentially correlative with the Mount Copleston volcanics. Late Ediacaran rifting in the northeastern Brooks Range is also broadly coincident with breakup of the Cordilleran margin as inferred from subsidence curves in the southern Canadian Rocky Mountains (Bond and Kominz, 1984) and a 569.6 ± 5.3 Ma U-Pb zircon age of synrift volcanic rocks in the Hamill Group (Colpron et al., 2002). However, Laurentian terminal Neoproterozoic deposits tend to be mixed carbonate-clastic sequences (e.g., Eisbacher, 1981; Miller, 1985). Conspicuously, the Katakturuk Dolomite lacks an equivalent of the Ediacaran Sheepbed Formation (Fig. 14), which is composed of organic-rich shales and siltstones. It should be noted that the Neoproterozoic strata of the northeastern Brooks Range are also distinct from those of Greenland and Svalbard, which both contain thick early Neoproterozoic carbonate-dominated successions overlain by ~300–400 m of Ediacaran shales (Halverson et al., 2004; Halverson et al., 2007b).

Thick sequences of platformal carbonates form preferentially at low latitudes due to the reverse solubility of carbonate can provide a rough paleolatitude constraint (Broeker and Peng, 1982). The lack of Ediacaran carbonate successions on Laurentia, for example, may be due to a mid- to high-latitude position for much of the middle Ediacaran (McCausland et al., 2007), whereas it is likely that the Arctic Alaska–Chukotka microplate was situated at low latitudes from the Cryogenian to the Late Ordovician. Paleomagnetic studies indicate that Siberia and many of the peri-Siberian terranes were also in the tropics

from the Neoproterozoic through the Ordovician (Cocks and Torsvik, 2007).

In matching apparent polar-wander (APW) paths, Pisarevsky et al. (2008) suggested that Siberia and Laurentia traveled together until at least the ca. 800 Ma breakup of Rodinia, but were separated by an additional landmass (potentially Arctidia, the Arctic Alaska–Chukotka microplate, and other peri-Siberian terranes). This reconstruction is followed in the Geodynamic Map of Rodinia (Li et al., 2007), which places the southeast margin of Siberia facing the northern margin of Laurentia (present coordinates) with ~1000 km of separation. Mafic dikes in southwestern Siberia have yielded Ar/Ar dates of 758 ± 4 Ma and 741 ± 4 Ma that could be correlative with the Mount Copleston volcanics and with the Franklin dikes, if errors are assumed in the Ar/Ar systematics (Gladkochub et al., 2006). A potential link also exists between unit K4 of the Katakturuk Dolomite and the Turkut Group in northwestern Siberia, which has a similar late Ediacaran rift history coupled with carbonate deposition and low-angle unconformities (Pelechaty et al., 1996). Not enough is known about the Neoproterozoic stratigraphy of the Taymir region and the northern margin of Siberia to assess a correlation (Pisarevsky and Natapov, 2003).

Detrital zircon histograms from beds below the Katakturuk Dolomite also share much in common with Neoproterozoic samples from the Farewell terrane, Laurentia, and Siberia, where 1100, 1380, 1465, 1880, 1980, 2025, 2065, 2680, and 2735 Ma peaks are also present (Rainbird et al., 1992; Rainbird et al., 1997; Khudoley et al., 2001; Bradley et al., 2007). There is one notable difference between these data sets: samples from unit O.G. and the Hula Hula diamictite contain several grains younger than 1000 Ma, whereas Neoproterozoic grains are absent from both the Siberian and Laurentian samples. The pre–1000 Ma ages in unit O.G. and the Hula Hula diamictite can possibly be explained by an older depositional age for many of the Laurentian and Siberian samples. These data support a Rodinian reconstruction with Siberia, Laurentia, and the Arctic Alaska–Chukotka microplate occupying adjacent positions. A scenario that is consistent with the detrital zircon, stratigraphic, and paleontological data is that Siberia and the Arctic Alaska–Chukotka microplate separated together from the northern margin of Laurentia in the early Neoproterozoic, and that Siberia and the Arctic Alaska–Chukotka microplate rifted apart in the late Ediacaran. This model can be tested with better age and stratigraphic characterizations of the rocks underlying the Turkut Group in northwestern Siberia, and with further paleomagnetic and geochronological studies on each of these margins.

The Opening of the Canada Basin

The rotation model for the origin of the Canada Basin predicts that the Katakturuk Dolomite is correlative with the early Neoproterozoic (pre–723 Ma) Shaler Supergroup of Amundson Basin. Chemostratigraphy, lithostratigraphy, and detrital zircon geochronology indicate that the Katakturuk Dolomite was instead deposited during the late Neoproterozoic (between ca. 760 and 542 Ma). However, there are no late Neoproterozoic rocks in the Amundsen Basin between the ca. 723 Ma Natkusiak Formation and the Cambrian Saline River Formation (Young, 1981). Thus, the simple rotation model is untenable with Neoproterozoic stratigraphy. If the rotation model is to be retained, it must be modified such that at least the North Slope subterrane portion of the Arctic Alaska–Chukotka microplate is an exotic block that docked on to the Canadian Arctic Islands sometime in the Phanerozoic. Sweeney (1982) proposed such a model in which the Arctic Alaska–Chukotka microplate arrived to a prerotation position in the late Paleozoic after over 1000 km of sinistral movement along the Canadian Arctic margin. If this docking of the North Slope subterrane occurred, it had to be during the Early to Middle Devonian, as there is no evidence of another orogeny on the Canadian Arctic margin until the late Cenozoic (Miall, 1976). A Devonian accretion would also reconcile Toro et al.'s (2004) ties in Carboniferous-Jurassic onlaps from the subsurface of the North Slope to Prince Patrick Island. However, the southward-directed mid-Devonian thrusting in the Brooks Range is inconsistent with this model (Oldow et al., 1987).

The close Paleozoic biogeographic ties between the North Slope subterrane and Siberia, and similarities between unit K4 and the Turkut Group, are consistent with a Lomonosov rifting model. In this model, the south-directed Early Devonian deformation could be a northern continuation of the Ellesmerian Orogeny (Oldow et al., 1987) through the hypothetical Arctidia continent. However, because little is known of the Neoproterozoic and Paleozoic stratigraphy of the submerged fragments of Arctidia and of the Taimyr Peninsula, the stratigraphic predictions of this model remain to be tested.

The fixed model for the opening of the Arctic predicts that the Katakturuk Dolomite is a northern continuation of the western Laurentian margin (Lane, 1997). While the Windermere Supergroup contains thick, late Neoproterozoic deposits, Ediacaran strata are dominated by clastics and separated from the northeastern Brooks Range by deep-water deposits in the British Mountains (Lane, 1991). Furthermore, the absence of Siberian fauna in Laurentia argues against a close connection between the Arctic Alaska–Chukotka microplate and Laurentia in the Paleozoic. Thus, a fixed model for the opening of the Canada Basin requires Ediacaran rifting and then reaccretion, perhaps in the Early Devonian.

Lastly, the original SAYBIA hypothesis (Johnston, 2001) can account for both the stratigraphic similarities between the Arctic Alaska–Chukotka microplate subterranes and the autochthonous Canadian Cordilleran terranes, and their similarities and differences with Laurentia. Particularly, the inferred subsidence history of the Katakturuk Dolomite (involving a failed Cryogenian rift and an active late Ediacaran rift) is similar to that of the Cordilleran margin and consistent with the idea that the Arctic Alaska–Chukotka microplate and the rest of SAYBIA rifted away from Laurentia. However, the exclusion of the North Slope subterrane with SAYBIA (Johnston, 2008) fails to explain the presence of peri-Siberian Paleozoic fauna on the North Slope subterrane (Blodgett et al., 2002; Dumoulin et al., 2002). Both iterations of the SAYBIA hypothesis can be tested with more detailed structural and stratigraphic studies on Neoproterozoic and Paleozoic strata in the North Slope and Hammond subterranes, in the Farewell and Alexander terranes, and in the Canadian Arctic Islands.

CONCLUSION

Detailed lithostratigraphic and chemostratigraphic studies coupled with detrital zircon geochronology suggest that: (1) the deposition of the Katakturuk Dolomite begins after an early-Cryogenian diamictite; (2) the Mount Copleston volcanics erupted after ca. 760 Ma and are partly coeval with the early-Cryogenian glaciations; (3) unit K2 is a basal Ediacaran cap carbonate; (4) units K2–K4 are Ediacaran in age; and (5) there is a large increase in sedimentation rate during the deposition of units K4 and N1, coupled with two low-angle unconformities. This latter observation could be the result of a late Ediacaran nonvolcanic rifting event. The Neoproterozoic stratigraphy, detrital zircon geochronology, and Paleozoic paleobiogeographic affinities of the North Slope subterrane indicate that the pre-Mississippian North Slope subterrane portion of the Arctic Alaska–Chukotka microplate was not simply connected to the Canadian Arctic islands. This contradicts the prevailing rotation model for the opening of the Arctic Oceans which calls for a Cretaceous formation of the Arctic Alaska–Chukotka microplate as it rifted away from North America and rotated 66° to its present position. If the Canada Basin formed through the rifting and rotation of the North Slope subterrane away from the Canadian Arctic islands, the rift occurred along a preexisting

Early to Middle Devonian suture between Laurentia and the exotic North Slope subterrane.

ACKNOWLEDGMENTS

We thank Julie Dumoulin, Adam Maloof, and Robert Rainbird for their thoughtful reviews. We thank field assistants Philip Kreycik and Ben Black for pushing through inclement weather and difficult terrain. We thank Greg Eischied for his assistance in Harvard's Paleoceanography Laboratory. We also thank Karla Knudson, Kevin Wecht, and Uyanga Bold for their help in the preparation of samples. We are grateful to Paul Hoffman and the National Science Foundation (NSF) Arctic Natural Science program for financial support, and VECO polar resources for logistics. We thank the Geological Society of America for a student research grant. Geochronologic studies were funded in part by NSF grant EAR-9423534 awarded to McClelland. We also thank Jim Clough, Paul Hoffman, Stephen Johnston, David Jones, and Taylor Stapleton for helpful discussions and comments throughout this work.

REFERENCES CITED

Aitken, J.D., 1981, Stratigraphy and sedimentology of the Upper Proterozoic Little Dal Group, Mackenzie Mountains, Northwest Territories, *in* Campbell, F.H.A., ed., Proterozoic basins of Canada: Geological Survey of Canada Paper 81-10, p. 47–71.

Aitken, J.D., 1991, The Ice Brook Formation and Post-Rapitan, Late Proterozoic glaciation, Mackenzie Mountains, Northwest Territories: Geological Survey of Canada Bulletin, v. 404, p. 1–43.

Allen, P.A., and Hoffman, P.F., 2005, Extreme winds and waves in the aftermath of a Neoproterozoic glaciation: Nature, v. 433, p. 123–127, doi: 10.1038/nature03176.

Amthor, J.E., Grotzinger, J.P., Schroeder, S., Bowring, S.A., Ramezani, J., Martin, M.W., and Matter, A., 2003, Extinction of Cloudina and Namacalathus at the Precambrian-Cambrian boundary in Oman: Geology, v. 31, no. 5, p. 431–434, doi: 10.1130/0091-7613(2003)031<0431:EOCANA>2.0.CO;2.

Anderson, M.M., and King, A.F., 1981, Precambrian tillites of the Conception Group on the Avalon Peninsula, southeastern Newfoundland, *in* Hambrey, M.J., and Harland, W.B., eds., Pre-Pleistocene glacial record on Earth: Cambridge, UK, Cambridge University Press, p. 760–763.

Babcock, L.E., Blodgett, R.B., and St. John, J., 1994, New Late (?) Proterozoic-age formations in the vicinity of Lone Mountain, McGrath Quadrangle, west-central Alaska, *in* Till, A.B., and Moore, T.E., eds., Geologic studies in Alaska by the U.S. Geological Survey, 1993: Washington, D.C., U.S. Government Printing Office, p. 143–155.

Bader, J. W., and Bird, K. J., 1986, Geologic map of the Demarcation Point, Mt. Michelson, Flaxman Island, and Barter Island Quadrangles, northeastern Alaska: U.S. Geological Survey Miscellaneous Investigations Series, Map I-1791.

Banner, J.L., and Hanson, G.N., 1990, Calculation of simultaneous isotopic and trace element variations during water-rock interaction with application to carbonate diagenesis: Geochimica et Cosmochimica Acta, v. 54, p. 3123–3137, doi: 10.1016/0016-7037(90)90128-8.

Bartley, J.K., and Kah, L.C., 2004, Marine carbon reservoir, C-org-C-carb coupling, and the evolution of the Proterozoic carbon cycle: Geology, v. 32, no. 2, p. 129–132, doi: 10.1130/G19939.1.

Black, L.P., Kamo, S.L., Allen, C.M., Davis, D.W., Aleinikoff, J.N., Valley, J.W., Mundil, R., Campbell, I.H., Korsch, R.J., Williams, I.S., and Foudoulis, C., 2004, Improved $^{206}Pb/^{238}U$ microprobe geochronology by the monitoring of a trace-element related matrix effect: SHRIMP, ID-TIMS, ELA-ICP-MS and oxygen isotope documentation for a series of zircon standards: Chemical Geology, v. 205, p. 115–140, doi: 10.1016/j.chemgeo.2004.01.003.

Blodgett, R.B., Clough, J.G., Dutro, J.T., Ormiston, A.R., Palmer, A.R., and Taylor, M.E., 1986, Age revisions of the Nanook Limestone and Katakturuk Dolomite, northeastern Brooks Range, Alaska, *in* Bartsch-Winkler, S., and Reed, K.M., eds., Geological studies in Alaska by the Geological Survey during 1985: U.S. Geological Survey Circular 978, p. 5–10.

Blodgett, R.B., Clough, J.G., Harris, A.G., and Robinson, M.S., 1992, The Mount Copleston Limestone, a new Lower Devonian Formation in the Shublik Mountains, northeastern Brooks Range, Alaska, *in* Bradley, D.C., and Ford, A.B., eds., Geological studies in Alaska by the U.S. Geological Survey, 1990: U.S. Geological Survey Bulletin 1999, p. 3–7.

Blodgett, R.B., Rohr, D.M., and Boucot, A.J., 2002, Paleozoic links among some Alaskan accreted terranes and Siberia based on megafossils, *in* Miller, E.L., Grantz, A., and Klemperer, S.L., eds., Tectonic evolution of the Bering Shelf–Chukchi Sea–Arctic Margin and adjacent landmasses: Boulder, Colorado, Geological Society of America Special Paper 360, p. 273–290.

Bond, G.C., and Kominz, M.A., 1984, Construction of tectonic subsidence curves for the early Paleozoic miogeocline, southern Canadian Rocky Mountains: Implications for subsidence mechanisms, age of breakup, and crustal thinning: Geological Society of America Bulletin, v. 95, no. 2, p. 155–173, doi: 10.1130/0016-7606(1984)95<155:COTSCF>2.0.CO;2.

Bowring, S.A., Myrow, P.M., Landing, E., and Ramezani, J., 2003, Geochronological constraints on terminal Neoproterozoic events and the rise of metazoans: Geophysical Research Abstracts, v. 5, p. 219.

Bowring, S.A., Grotzinger, J.P., Condon, D.J., Ramezani, J., and Newall, M., 2007, Geochronologic constraints on the chronostratigraphic framework of the Neoproterozoic Huqf Supergroup, Sultanate of Oman: American Journal of Science, v. 307, p. 1097–1145.

Bradley, D.C., Dumoulin, J.A., Blodgett, R.B., Harris, A.G., Roeske, S.M., McClelland, W.C., and Layer, P.W., 2006, Geology and affinity of Alaska's Farewell terrane: Geological Society of America Abstracts with Programs, v. 38, p. 12.

Bradley, D.C., McClelland, W.C., Wooden, D., Till, A.B., Roeske, S.M., Miller, M.L., Karl, S.M., and Abbott, G., 2007, Detrital zircon geochronology of some Neoproterozoic to Triassic rocks in interior Alaska, *in* Ridgway, K.D., Trop, J.M., and ONeill, J.M., eds., Tectonic growth of a collisional continental margin: Crustal evolution of southern Alaska: Geological Society of America Special Paper 431, p. 155–190.

Brand, U., and Veizer, J., 1981, Chemical diagenesis of a multicomponent carbonate system—1: Stable isotopes: Journal of Sedimentary Petrology, v. 51, p. 987–997.

Brasier, M.D., Shields, G., Kuleshov, V.N., and Zhegallo, E.A., 1996, Integrated chemo- and biostratigraphic calibration of early animal evolution: Neoproterozoic–early Cambrian of southwest Mongolia: Geological Magazine, v. 133, no. 4, p. 445–485.

Broeker, W.S., and Peng, T.H., 1982, Tracers in the sea: Palisades, New York, Lamont-Doherty Earth Observatory Press.

Burns, S.J., and Matter, A., 1993, Carbon isotopic record of the Latest Proterozoic from Oman: Eclogae Geologicae Helvetiae, v. 86, no. 2, p. 595–607.

Carey, S.W., 1955, The orocline concept in geotectonics: Royal Society of Tasmania Proceedings, v. 89, p. 255–288.

Carey, S.W., 1958, Continental Drift, *in* Carey, S.W., ed., Continental drift: A symposium: Hobart, Australia, University of Tasmania, p. 177–355.

Chang, Z., Vervoort, J.D., McClelland, W.C., and Knaack, C., 2006, U-Pb dating of zircon by LA-ICP-MS: Geochemistry Geophysics Geosystems, v. 7, p. Q05009, doi: 10.1029/2005GC001100.

Churkin, M.J., Jr., and Trexler, J.H.J., 1980, Circum-Arctic plate accretion—Isolating part of a Pacific plate to form the nucleus of the Arctic Basin: Earth and Planetary Science Letters, v. 48, p. 356–362, doi: 10.1016/0012-821X(80)90199-5.

Cloud, P.E., Jr., and Glaessner, M.F., 1982, The Ediacaran period and system: Metazoa inherit the Earth: Science, v. 217, p. 783–792, doi: 10.1126/science.217.4562.783.

Clough, J.G., 1989, General stratigraphy of the Katakturuk Dolomite in the Sadlerochit and Shublik Mountains, Arctic National Wildlife Refuge, northeastern Alaska: Alaska Division of Geological and Geophysical Surveys, Public Data File 89-4a, p. 1–11.

Clough, J.G., and Goldhammer, R.K., 2000, Evolution of the Neoproterozoic Katakturuk dolomite ramp complex, northeastern Brooks Range, Alaska, *in* Grotzinger, J.P., and James, N.P., eds., Carbonate sedimentation and diagenesis in the evolving Precambrian world: Tulsa, Oklahoma, SEPM (Society of Sedimentary Geology) Special Publication, no. 67, p. 209–241.

Clough, J.G., Robinson, M.S., Pessel, M.S., Imm, G.H., Blodgett, R.B., Harris, A.G., Bergman, S.C., and Foland, K.A., 1990, Geology and age of Franklinian and older rocks in the Sadlerochit and Shublik Mountains, Arctic National Wildlife Refuge, Alaska: Geological Association of Canada and Mineralogical Association of Canada, Annual Meeting, Program with Abstracts, v. 15, p. A25.

Cochran, J.R., Edwards, M.H., and Coakley, B.J., 2006, Morphology and structure of the Lomonosov Ridge, Arctic Ocean: Geochemistry Geophysics Geosystems, v. 7.

Cocks, L., and Torsvik, T.H., 2007, Siberia, the wandering northern terrane, and its changing geography through the Paleozoic: Earth-Science Reviews, v. 82, no. 1–2, p. 29–74, doi: 10.1016/j.earscirev.2007.02.001.

Colpron, M., Logan, J.M., and Mortensen, J.K., 2002, U-Pb zircon age constraint for late Neoproterozoic rifting and initiation of the lower Paleozoic passive margin of western Laurentia: Canadian Journal of Earth Sciences, v. 39, p. 133–143, doi: 10.1139/e01-069.

Colpron, M., Nelson, J.L., and Murphy, D.C., 2007, Northern Cordilleran terranes and their interactions through time: GSA Today, v. 17, no. 4/5, p. 4–10, doi: 10.1130/GSAT01704-5A.1.

Condon, D.J., Zhu, M., Bowring, S.A., Wang, W., Yang, A., and Jin, Y., 2005, U-Pb ages from the Neoproterozoic Doushantuo Formation, China: Science, v. 308, p. 95–98, doi: 10.1126/science.1107765.

Corkeron, M., 2007, "Cap carbonates" and Neoproterozoic glacigenic successions from the Kimberley region, northwest Australia: Sedimentology, v. 54, p. 871–903, doi: 10.1111/j.1365-3091.2007.00864.x.

Corsetti, F.A., and Grotzinger, J.P., 2005, Origin and significance of tube structures in Neoproterozoic post-glacial cap carbonates: Example from Noonday Dolomite, Death Valley, United States: Palaios, v. 20, p. 348–363, doi: 10.2110/palo.2003.p03-96.

Cozzi, A., Grotzinger, J.P., and Allen, P.A., 2004, Evolution of a terminal Neoproterozoic carbonate ramp system (Buah Formation, Sultanate of Oman): Effects of basement paleotopography: Geological Society of America Bulletin, v. 116, no. 11/12, p. 1367–1384, doi: 10.1130/B25387.1.

Crimes, T.P., 1992, The record of trace fossils across the Proterozoic-Cambrian boundary, *in* Lipps, J.H., and Signor, P.W., III, eds., Origin and early evolution of the Metazoa: New York, Plenum, p. 177–202.

Dilliard, K.A., Pope, M., Coniglio, M., Hasiotis, S.T., and Lieberman, B.S., 2007, Stable isotope geochemistry of the lower Cambrian Sekwi Formation, Northwest Territories, Canada: Implications for ocean chemistry and secular curve generation: Palaeogeography, Palaeoclimatology, Palaeoecology, v. 256, p. 174–194, doi: 10.1016/j.palaeo.2007.02.031.

Dumoulin, J.A., 1988, Stromatolite- and coated-grain-bearing carbonate rocks of the western Brooks Range, *in* Galloway, J.P., and Hamilton, T.D., eds., Geologic studies in Alaska by the U.S. Geological Survey during 1987: Washington, D.C., U.S. Government Printing Office, p. 31–34.

Dumoulin, J.A., and Harris, A.G., 1994, Depositional framework and regional correlation of pre-Carboniferous metacarbonate rocks of the Snowden Mountain area, Central Brooks Range, northern Alaska: U.S. Geological Survey Professional Paper 1545, p. 1–55.

Dumoulin, J.A., Harris, A.G., Bradley, D.C., and de Freitas, T.A., 1998, Facies patterns and conodont biogeography in Arctic Alaska and the Canadian Arctic Islands: Evidence against the juxtaposition of these areas during Early Paleozoic time: Polarforschung, v. 68, p. 257–266.

Dumoulin, J.A., Harris, A.G., Gagiev, M., Bradley, D.C., and Repetski, J.E., 2002, Lithostratigraphic, conodont, and other faunal links between lower Paleozoic strata

in northern and central Alaska and northeastern Russia, *in* Miller, E.L., Grantz, A., and Klemperer, S.L., eds., Tectonic evolution of the Bering Shelf–Chukchi Sea–Arctic Margin and adjacent landmasses: Boulder, Colorado, Geological Survey of America Special Paper 360, p. 291–312.

Dutro, J.T., 1970, Pre-Carboniferous carbonate rocks, northeastern Alaska, *in* Proceedings of the Geological Seminar on the North Slope of Alaska: Los Angeles, California, American Association of Petroleum Geologists, Pacific Section, p. M1–M8.

Dutro, J.T., 1981, Geology of Alaska bordering the Arctic Ocean, *in* Nairn, A.E.M., Churkin, M. J., and Stehli, F.T., eds., The ocean basins and margins: The Arctic Ocean: New York, Plenum, p. 21–36.

Eberli, G.P., and Ginsburg, R.N., 1989, Aggrading and prograding infill of buried Cenozoic seaways, northwestern Great Bahama Bank, *in* Crevello, P.D., Sarg, J.F., Wilson, J.L., and Read, J.F., eds., Controls on carbonate platform and basin evolution, Society of Economic Paleontologists and Mineralogists Special Publication, p. 339–355.

Eisbacher, G.H., 1981, Sedimentary tectonics and glacial record in the Windermere Supergroup, Mackenzie Mountains, northwestern Canada: Geological Survey of Canada Paper 80-27, p. 1–40.

Embry, A.F., 1989, Correlation of Upper Paleozoic and Mesozoic sequences between Svalbard, Canadian Arctic Archipelago and northern Alaska, *in* Collinson, J.D., ed., Correlation in hydrocarbon exploration: Stavanger, Norway, Norwegian Petroleum Society, p. 89–98.

Embry, A.F., and Dixon, J., 1990, The breakup unconformity of the Amerasia Basin, Arctic Ocean: Evidence from Arctic Canada: Geological Society of America Bulletin, v. 102, p. 1526–1534, doi: 10.1130/0016-7606(1990)102<1526:TBUOTA>2.3.CO;2.

Evans, D.A.D., 2000, Stratigraphic, geochronological, and paleomagnetic constraints upon the Neoproterozoic climatic paradox: American Journal of Science, v. 300, p. 347–433, doi: 10.2475/ajs.300.5.347.

Fanning, C.M., and Link, P.K., 2004, U-Pb SHRIMP ages of Neoproterozoic (Sturtian) glaciogenic Pocatello Formation, southeastern Idaho: Geology, v. 32, p. 881–884, doi: 10.1130/G20609.1.

Fedonkin, M.A., and Waggoner, B.M., 1997, The late Precambrian fossil *Kimberella* is a mollusc-like bilaterian organism: Nature, v. 388, p. 868, doi: 10.1038/42242.

Fike, D.A., Grotzinger, J.P., Pratt, L.M., and Summons, R.E., 2006, Oxidation of the Ediacaran Ocean: Nature, v. 444, p. 744–747, doi: 10.1038/nature05345.

Frimmel, H.E., Klotzli, U.S., and Siegfried, P.R., 1996, New Pb-Pb single zircon age constraints on the timing of Neoproterozoic glaciation and continental break-up in Namibia: The Journal of Geology, v. 104, p. 459–469.

Fuis, G.S., Moore, T.E., Plafker, G., Brocher, T.M., Fisher, M.A., Mooney, W.D., Nokleberg, W.J., Page, R.A., Beaudoin, B.C., Christensen, N.I., Levander, A.R., Lutter, W.J., Saltus, R.W., and Ruppert, N.A., 2008, Trans-Alaska crustal transect and continental evolution involving subduction underplating and synchronous foreland thrusting: Geology, v. 36, no. 3, p. 267–270, doi: 10.1130/G24257A.1.

Gladkochub, D.P., Wingate, M.T.D., Pisarevsky, S.A., Donskaya, T.V., Mazukabzov, A.M., Ponomarchuk, V.A., and Stanevich, A.M., 2006, Mafic intrusions in southwestern Siberia and implications for a Neoproterozoic connection with Laurentia: Precambrian Research, v. 147, p. 260–278, doi: 10.1016/j.precamres.2006.01.018.

Glaessner, M.F., and Wade, M., 1966, The late Precambrian fossils from Ediacara, South Australia: Palaeontology, v. 9, p. 599–628.

Goldring, W., 1938, Algal barrier reefs in the Lower Ozarkian of New York: New York State Museum Bulletin, v. 315, p. 0–75.

Grantz, A., and May, S.D., 1983, Rifting history and structural development of the continental margin north of Alaska, *in* Watkins, J.S., and Drake, C.L., eds., Studies in continental margin geology: American Association of Petroleum Geologists Memoir 34, p. 77–100.

Grantz, A., Eittreim, S., and Dinter, D.A., 1979, Geology and tectonic development of the continental margin north of Alaska: Tectonophysics, v. 59, p. 263–291, doi: 10.1016/0040-1951(79)90050-7.

Grantz, A., Moore, T.E., and Roeske, S.M., 1991, A-3 Gulf of Alaska to Arctic Ocean: Boulder, Colorado, Geological Society of America Centennial Continental/Ocean Transect no. 15, p. 1–72.

Grantz, A., Clark, D.L., Phillips, R.L., and Srivastava, S.P., 1998, Phanerozoic stratigraphy of Northwind Ridge, magnetic anomalies in the Canada basin, and the geometry and timing of rifting in the Amerasia basin, Arctic Ocean: Geological Society of America Bulletin, v. 110, p. 801–820, doi: 10.1130/0016-7606(1998)110<0801:PSONRM>2.3.CO;2.

Grey, K., 2005, Ediacaran palynology of Australia: Memoir 31 of the Association of Australian Paleontologists, 439 p.

Grey, K., Walter, M.R., and Calver, C.R., 2003, Neoproterozoic biotic diversification: Snowball Earth or aftermath of the Acraman impact?: Geology, v. 31, no. 5, p. 459–462, doi: 10.1130/0091-7613(2003)031<0459:NBDSEO>2.0.CO;2.

Grotzinger, J.P., Bowring, S.A., Saylor, B.Z., and Kaufman, A.J., 1995, Biostratigraphic and geochronologic constraints on early animal evolution: Science, v. 270, no. 5236, p. 598–604, doi: 10.1126/science.270.5236.598.

Halgedahl, L.L., and Jarrard, R.D., 1987, Paleomagnetism of the Kuparuk River Formation from oriented drill core: Evidence for rotation of the Arctic Alaska plate, *in* Tailleur, I., and Weimer, P., eds., Alaskan North Slope geology, Book 50: Santa Barbara, California, Society of Economic Paleontologists and Mineralogists, Pacific Section, p. 581–617.

Halverson, G.P., Hoffman, P.F., Schrag, D.P., and Kaufman, A.J., 2002, A major perturbation of the carbon cycle before the Ghaub glaciation (Neoproterozoic) in Namibia: Prelude to snowball Earth?: Geochemistry Geophysics Geosystems, v. 3.

Halverson, G.P., Maloof, A.C., and Hoffman, P.F., 2004, The Marinoan glaciation (Neoproterozoic) in northeast Svalbard: Basin Research, v. 16, p. 297–324, doi: 10.1111/j.1365-2117.2004.00234.x.

Halverson, G.P., Hoffman, P.F., Schrag, D.P., Maloof, A.C., and Rice, A.H.N., 2005, Toward a Neoproterozoic composite carbon-isotope record: Geological Society of America Bulletin, v. 117, no. 9–10, p. 1181–1207, doi: 10.1130/B25630.1.

Halverson, G.P., Dudás, F.O., Maloof, A.C., and Bowring, S.A., 2007a, Evolution of the $^{87}Sr/^{86}Sr$ composition of Neoproterozoic Seawater: Palaeogeography, Palaeoclimatology, Palaeoecology, v. 256, p. 103–129, doi: 10.1016/j.palaeo.2007.02.028.

Halverson, G.P., Maloof, A.C., Schrag, D.P., Dudas, F.O., and Hurtgen, M.T., 2007b, Stratigraphy and geochemistry of a ca 800 Ma negative carbon isotope interval in northeastern Svalbard: Chemical Geology, v. 237, p. 5–27, doi: 10.1016/j.chemgeo.2006.06.013.

Hambrey, M.J., and Harland, W.B., 1981, Earth's Pre-Pleistocene Glacial Record: London, Cambridge University Press, p. 1004.

Hamilton, W., 1970, The Uralides and the motion of the Russian and Siberian Platforms: Geological Society of America Bulletin, v. 81, p. 2553–2576, doi: 10.1130/0016-7606(1970)81[2553:TUATMO]2.0.CO;2.

Hanks, C.R., 1991, A comparative study of contrasting structural styles in the range-front region of the North [Ph.D. thesis]: Fairbanks, Alaska, Geology and Geophysics Department, University of Alaska, 336 p.

Harland, W.B., 1964, Evidence of late Precambrian glaciation and its significance, *in* Nairn, A.E.M., ed., Problems in palaeoclimatology: London, UK, Interscience, p. 119–149.

Harris, A.G., Lane, R.H., and Tailleur, I.L., 1990, Conodont thermal maturation patterns in Paleozoic and Triassic rocks, northern Alaska—Geological and exploration implications, *in* Grantz, A., Johnshon, L., and Sweeney, J.F., eds., The Arctic Ocean region: Geological Society of America, Decade of North American Geology, Series L, p. 181–191.

Heaman, L.M., LeCheminant, A.N., and Rainbird, R.H., 1992, Nature and timing of Franklin igneous events, Canada: Implications for a Late Proterozoic mantle plume and the break-up of Laurentia: Earth and Planetary Science Letters, v. 109, p. 117–131, doi: 10.1016/0012-821X(92)90078-A.

Hillhouse, J.W., and Grommé, C.S., 1983, Paleomagnetic studies and the hypothetical rotation of Arctic Alaska: Journal of the Alaska Geological Society, v. 2, p. 27–39.

Hoffman, P.F., 1967, Algal stromatolites: use in stratigraphic correlation and paleo-current determination: Science, v. 157, no. 3792, p. 1043–1045, doi: 10.1126/science.157.3792.1043.

Hoffman, P.F., 1991, Did the Breakout of Laurentia Turn Gondwanaland Inside-Out?: Science, v. 252, no. 5011, p. 1409–1412, doi: 10.1126/science.252.5011.1409.

Hoffman, P.F., and Schrag, D.P., 2002, The snowball Earth hypothesis: Testing the limits of global change: Terra Nova, v. 14, no. 3, p. 129–155, doi: 10.1046/j.1365-3121.2002.00408.x.

Hoffman, P.F., Kaufman, A.J., and Halverson, G.P., 1998a, Comings and goings of global glaciations on a Neoproterozoic tropical platform in Namibia: GSA Today, v. 8, no. 5, p. 1–9.

Hoffman, P.F., Kaufman, A.J., Halverson, G.P., and Schrag, D.P., 1998b, A Neoproterozoic snowball Earth: Science, v. 281, p. 1342–1346, doi: 10.1126/science.281.5381.1342.

Hoffmann, K.H., Condon, D.J., Bowring, S.A., and Crowley, J.L., 2004, U-Pb zircon date from the Neoproterozoic Ghaub Formation, Namibia: Constraints on Marinoan glaciation: Geology, v. 32, p. 817–820, doi: 10.1130/G20519.1.

Hoffman, P.F., Halverson, G.P., Domack, E.W., Husson, J.M., Higgins, J.A., and Schrag, D.P., 2007, Are basal Ediacaran (635 Ma) post-glacial "cap dolostones" diachronous?: Earth and Planetary Science Letters, v. 258, p. 114–131, doi: 10.1016/j.epsl.2007.03.032.

Hotinski, R.M., Kump, L.R., and Arthur, M., 2004, The effectiveness of the Paleoproterozoic biological pump: A $\delta^{13}C$ gradient from platform carbonates of the Pethei Group (Great Slave Lake Supergroup, NWT): Geological Society of America Bulletin, v. 116, no. 5/6, p. 539–554, doi: 10.1130/B25272.1.

Jacobsen, S., and Kaufman, A.J., 1999, The Sr, C, and O isotopic evolution of Neoproterozoic seawater: Chemical Geology, v. 161, p. 37–57, doi: 10.1016/S0009-2541(99)00080-7.

James, N.P., Narbonne, G.M., and Kyser, K.T., 1999, Neoproterozoic cap carbonate facies: Mackenzie Mountains, NW Canada: Abiotic precipitation and global glacial meltdown: Geological Society of America Abstracts with Programs, v. 31, p. 487.

James, N.P., Narbonne, G.M., and Kyser, T.K., 2001, Late Neoproterozoic cap carbonates: Mackenzie Mountains, northwestern Canada: Precipitation and global glacial meltdown: Canadian Journal of Earth Sciences, v. 38, no. 8, p. 1229–1262, doi: 10.1139/cjes-38-8-1229.

Jiang, G., Kennedy, M.J., and Christie-Blick, N., 2003, Stable isotopic evidence for methane seeps in Neoproterozoic postglacial cap carbonates: Nature, v. 426, p. 822–826, doi: 10.1038/nature02201.

Johnston, S.T., 2001, The great Alaskan terrane wreck: Reconciliation of paleomagnetic and geological data in the northern Cordillera: Earth and Planetary Science Letters, v. 193, p. 259–272, doi: 10.1016/S0012-821X(01)00516-7.

Johnston, S.T., 2008, The Cordilleran Ribbon Continent of North America: Annual Review of Earth and Planetary Sciences, v. 36, p. 495–530, doi: 10.1146/annurev.earth.36.031207.124331.

Jones, P.B., 1980, Evidence from Canada and Alaska on plate tectonic evolution of the Arctic Ocean Basin: Nature, v. 285, p. 215–217, doi: 10.1038/285215a0.

Julian, F.E., and Oldow, J.S., 1998, Structure and lithology of the lower Paleozoic Apoon assemblage, eastern Doonerak window, central Brooks Range, Alaska, *in* Oldow, J.S., and Lallemant, A., eds., Architecture of the central Brooks Range fold and thrust belt, Arctic Alaska: Boulder, Colorado, Geological Society of America Special Paper 324, p. 65–80.

Kaufman, A.J., and Knoll, A.H., 1995, Neoproterozoic variations in the C-isotopic composition of seawater: Stratigraphic and biogeochemical implications: Neoproterozoic stratigraphy and Earth history, v. 73, no. 1–4, p. 27–49.

Kaufman, A.J., Knoll, A.H., Semikhatov, M.A., Grotzinger, J.P., Jacobsen, S.B., and Adams, W., 1996, Integrated

chronostratigraphy of Proterozoic-Cambrian boundary beds in the western Anabar region, northern Siberia: Geological Magazine, v. 133, no. 5, p. 509–533.

Kendall, C.G.S.C., and Warren, J., 1987, A review of the origin and setting of teepees and their associated fabrics: Sedimentology, v. 34, no. 6, p. 1007–1027, doi: 10.1111/j.1365-3091.1987.tb00590.x.

Kennedy, M.J., 1996, Stratigraphy, sedimentology, and isotope geochemistry of Australian Neoproterozoic postglacial cap dolostones: Deglaciation, $\delta^{13}C$ excursions, and carbonate precipitation: Journal of Sedimentary Research, v. 66, p. 1050–1064.

Kerr, J.W., 1981, Evolution of the Canadian Arctic Islands: A transition between the Atlantic and Arctic oceans, *in* Nairn, A.E.M., Churkin, M.J., and Stehli, F.G., eds., Ocean basins and margins: The Arctic Ocean: New York, Plenum, p. 105–199.

Khudoley, A.K., Rainbird, R.H., Stern, R.A., Kropachev, A.P., Heaman, L.M., Zann, A.M., Podkovyrov, V.N., Belova, V.N., and Sukhorukov, V.I., 2001, Sedimentary evolution of the Riphean-Vendian basin of southeastern Siberia: Precambrian Research, v. 111, p. 129–163, doi: 10.1016/S0301-9268(01)00159-0.

Knoll, A.H., Hayes, J.M., Kaufman, A.J., Swett, K., and Lambert, I.B., 1986, Secular variation in carbon isotope ratios from Upper Proterozoic successions of Svalbard and East Greenland: Nature, v. 321, p. 832–838, doi: 10.1038/321832a0.

Knoll, A.H., and Swett, K., 1990, Carbonate deposition during the late Proterozoic era: An example from Spitsbergen: Proterozoic evolution and environments, v. 290-A, p. 104–132.

Knoll, A.H., and Walter, M.R., 1992, Latest Proterozoic stratigraphy and Earth history: Nature, v. 356, p. 673–677, doi: 10.1038/356673a0.

Kouchinsky, A., Bengtson, S., Pavlov, V., Runnegar, B., Trorssander, P., Young, E., and Ziegler, K., 2007, Carbon isotope stratigraphy of the Precambrian-Cambrian Sukharikha River section, northwestern Siberian platform: Geological Magazine, v. 144, no. 4, p. 609–618, doi: 10.1017/S0016756807003354.

Kroopnick, P.M., 1985, The distribution of ^{13}C and ΣCO_2 in the world oceans: Deep-Sea Research, v. 32, p. 57–84, doi: 10.1016/0198-0149(85)90017-2.

Kump, L.R., and Arthur, M., 1999, Interpreting carbon-isotope excursions: Carbonates and organic matter: Chemical Geology, v. 161, p. 181–198, doi: 10.1016/S0009-2541(99)00086-8.

Lane, L.S., 1991, The pre-Mississippian "Neruokpuk Formation," northeastern Alaska and northwestern Yukon: Review and new regional correlation: Canadian Journal of Earth Sciences, v. 28, p. 1521–1533.

Lane, L.S., 1997, Canada Basin, Arctic Ocean: Evidence against a rotational origin: Tectonics, v. 16, p. 363–387, doi: 10.1029/97TC00432.

Lane, L.S., 1998, "Fixist" origin for Arctic Alaska: The Rodinia reconstruction: Celle, Germany, III International Conference on Arctic Margins, p. 107–108.

Lawver, L.A., and Scotese, C.R., 1990, A review of tectonic models for the evolution of the Canada Basin, *in* Grantz, A., Johnston, L., and Sweeney, J.F., eds., The geology of North America, Volume L: Boulder, Colorado, Geological Society of America, p. 593–618.

Leffingwell, E., 1919, The Canning River region, northern Alaska: U.S. Geological Survey Professional Paper 109, v. 109.

Li, Z.X., Bogdanova, S.V., Collins, A.S., Davidson, A., De Waele, B., Ernst, R.E., Fitzsimons, I. C.W., Fuck, R.A., Gladkochub, D.P., Jacobs, J., Karlstrom, K.E., Lu, S., Natapov, L.M., Pease, V., Pisarevsky, S.A., Thrane, K., and Vernikovsky, V., 2008, Assembly, configuration, and break-up history of Rodinia: A synthesis: Precambrian Research, v. 160, no. 1–2, p. 179–210, doi: 10.1016/j.precamres.2007.04.021.

Logan, G.A., Hayes, J.M., Hieshima, G.B., and Summons, R.E., 1995, Terminal Proterozoic reorganization of biogeochemical cycles: Nature, v. 376, p. 53–56, doi: 10.1038/376053a0.

Ludwig, K.R., 2003, User's manual for Isoplot 3.00: a geochronological toolkit for Microsoft Excel: Berkeley Geochronology Center Special Publication, v. 4, p. 1–70.

Maloof, A.C., Schrag, D.P., Crowley, J.L., and Bowring, S.A., 2005, An expanded record of Early Cambrian carbon cycling from the Anti-Atlas Margin, Morocco: Canadian Journal of Earth Sciences, v. 42, no. 12, p. 2195–2216, doi: 10.1139/e05-062.

Martin, M.W., Grazhdankin, D.V., Bowring, S.A., Fedonkin, M.A., and Kirschvink, J.L., 2000, Age of Neoproterozoic bilatarian body and trace fossils, White Sea, Russia: Implications for Metazoan evolution: Science, v. 288, no. 5467, p. 841–845, doi: 10.1126/science.288.5467.841.

Mayfield, C.F., Tailleur, I., and Ellersieck, I., 1988, Stratigraphy, structure, and palinspastic synthesis of the western Brooks Range, northwestern Alaska, *in* Gryc, G., ed., Geology and exploration of the National Petroleum Reserve in Alaska, 1974 to 1982: U.S. Geological Survey Professional Paper 1399, p. 143–186.

McCausland, P.J.A., Van der Voo, R., and Hall, C.M., 2007, Circum-Iapetus paleogeography of the Precambrian-Cambrian transition with a new paleomagnetic constraint from Laurentia: Precambrian Research, v. 156, p. 125–152, doi: 10.1016/j.precamres.2007.03.004.

McClelland, W.C., 1997, Detrital zircon studies of the Proterozoic Neruokpuk Formation, Sadlerochit and Franklin Mountains, northern Alaska: Geological Society of America Abstracts with Programs, v. 25, no. 5, p. 28.

McClelland, W.C., and Mattinson, J.M., 1996, Resolving high precision ages from Tertiary plutons with complex zircon systematics: Geochimica et Cosmochimica Acta, v. 60, p. 3955–3965, doi: 10.1016/0016-7037(96)00214-1.

McFadden, K.A., Huang, J., Chu, X., Jiang, G., Kaufman, A.J., Zhou, C., Yuan, X., and Xiao, S., 2008, Pulsed oxidation and biological evolution in the Ediacaran Doushantuo Formation: Proceedings of the National Academy of Sciences of the United States of America, v. 105, no. 9, p. 3197–3202, doi: 10.1073/pnas.0708336105.

McKirdy, D.M., Burgess, J.M., Lemon, N.M., Yu, X., Cooper, A.M., Gostin, V.A., Jenkins, R.J.F., and Both, R.A., 2001, A chemostratigraphic overview of the late Cryogenian interglacial sequence in the Adelaide fold-thrust belt, South Australia: Precambrian Research, v. 106, p. 149–186, doi: 10.1016/S0301-9268(00)00130-3.

Miall, A.D., 1976, Devonian geology of Banks Island, Arctic Canada, and its bearing on the tectonic development of the circum-Arctic region: Geological Society of America Bulletin, v. 87, p. 1599–1608, doi: 10.1130/0016-7606(1976)87<1599:DGOBIA>2.0.CO;2.

Miller, E.L., Toro, J., Gehrels, G., Amato, J.M., Prokopiev, A., Tuchkova, M.I., Akinin, V.V., Dumitru, T.A., Moore, T.E., and Cecile, M.P., 2006, New insights into Arctic paleogeography and tectonics from U-Pb detrital zircon geochronology: Tectonics, v. 25, TC3013, doi:10.1029/2005TC001830.

Miller, J.M.G., 1985, Glacial and syntectonic sedimentation: The upper Proterozoic Kinston Peak Formation, southern Panamint Range, eastern California: Geological Society of America Bulletin, v. 96, p. 75–85.

Moore, T.E., 1987, Geochemistry and tectonic setting of some volcanic rocks of the Franklinian assemblage, central and eastern Brooks Range, *in* Tailleur, I., and Weimer, P., eds., Alaskan North Slope geology: Society of Economic Paleontologists and Mineralogists, Pacific Section, p. 691–710.

Moore, T.E., Wallace, W.K., Bird, K.J., Karl, S.M., Mull, C.G., and Dillon, J.T., 1994, The geology of northern Alaska, *in* Phlafker, G., and Berg, H.C., eds., The geology of North America, Volume G-1, The geology of Alaska: Boulder, Colorado, Geological Society of America, p. 49–140.

Moore, T.E., Wallace, W.K., Mull, C.G., Adams, K.E., Plafker, G., and Nokleberg, W.J., 1997, Crustal implications of bedrock geology along the Trans-Alaska Crustal Transect (TACT) in the Brooks Range, northern Alaska: Tectonics, v. 102, no. B9, p. 20,645–20,684.

Muehlenbachs, K., 1998, The oxygen isotopic composition of the oceans, sediments and the seafloor: Chemical Geology, v. 145, no. 3–4, p. 263–273, doi: 10.1016/S0009-2541(97)00147-2.

Muehlenbachs, K., and Clayton, R., 1976, Oxygen isotopic composition of the oceanic crust and its bearing on seawater: Journal of Geophysical Research, v. 81, no. 23, p. 4365–4369, doi: 10.1029/JB081i023p04365.

Myrow, P.M., and Kaufman, A.J., 1999, A newly discovered cap carbonate above Varanger-age glacial deposits in Newfoundland, Canada: Journal of Sedimentary Research, v. 69, p. 784–793.

Oldow, J.S., Lallemant, A., Julian, F.E., and Seidensticker, C.M., 1987, Ellesmerian (?) and Brookian deformation in the Franklin Mountains, northeastern Brooks Range, Alaska, and its bearing on the origin of the Canada Basin: Geology, v. 15, p. 37–41, doi: 10.1130/0091-7613(1987)15<37:EABDIT>2.0.CO;2.

O'Neil, J.R., Clayton, R.N., and Mayeda, T.K., 1969, Oxygen isotope fractionation between divalent metal carbonates: The Journal of Chemical Physics, v. 51, p. 5547–5558, doi: 10.1063/1.1671982.

Ostenso, N.A., 1974, Arctic ocean margins, *in* Burk, C.A., and Drake, C.L., eds., The geology of continental margins: New York, Springer-Verlag, p. 753–763.

Paces, J.B., and Miller, J.D.J., 1993, Precise U-Pb ages of Duluth complex and related mafic intrusions, northeastern Minnesota: Geochronological insights to physical, petrogenetic, paleomagnetic, and tectonomagmatic processes associated with the 1.l Ga midcontinent rift system: Journal of Geophysical Research, v. 98-B8, p. 13,997–14,014.

Patrick, B.E., and McClelland, W.C., 1995, Late Proterozoic granitic magmatism on Seward Peninsula and a Barentian origin for Arctic Alaska–Chukotka: Geology, v. 23, no. 1, p. 81–84, doi: 10.1130/0091-7613(1995)023<0081:LPGMOS>2.3.CO;2.

Pelechaty, S.M., 1998, Integrated chronostratigraphy of the Vendian System of Siberia: Implications for a global stratigraphy: Journal of the Geological Society, v. 155, p. 957–973, doi: 10.1144/gsjgs.155.6.0957.

Pelechaty, S.M., Grotzinger, J.P., Kashirtsev, V.A., and Zhernovsky, V.P., 1996, Chemostratigraphic and sequence stratigraphic constraints on Vendian-Cambrian Basin dynamics, northeast Siberian Craton: The Journal of Geology, v. 104, p. 543–563.

Pell, S.D., McKirdy, D.M., Jansyn, J., and Jenkins, R.J.F., 1993, Ediacaran carbon isotope stratigraphy of South Australia—An initial study: Transactions of the Royal Society of South Australia, v. 117, p. 153–161.

Persits, F.M., and Ulmishek, G.F., 2003, Maps showing geology, oil and gas fields, and geological provinces of the Arctic: U.S. Geological Survey Open-File Report 97-470-J.

Peryt, T.M., Hoppe, A., Bechstadt, T., Koster, J., Pierre, C., and Richter, D.K., 1990, Late Proterozoic aragonitic cement crusts, Bambui Group, Minas Gerais, Brazil: Sedimentology, v. 37, p. 279–286, doi: 10.1111/j.1365-3091.1990.tb00959.x.

Pisarevsky, S.A., and Natapov, L.M., 2003, Siberia and Rodinia: Tectonophysics, v. 375, p. 221–245, doi: 10.1016/j.tecto.2003.06.001.

Pisarevsky, S.A., Natapov, L.M., Donskaya, T.V., Gladkochub, D.P., and Vernikovsky, V., 2008, Proterozoic Siberia: A promontory of Rodina: Precambrian Research, v. 160, no. 1–2, p. 66–76, doi: 10.1016/j.precamres.2007.04.016.

Pruss, S.B., and Corsetti, F.A., 2002, Unusual aragonite precipitates in the Neoproterozoic Rainstorm Member of the Johnnie Formation, *in* Corsetti, F.A., ed., Proterozoic-Cambrian of the Great Basin and beyond Society of Economic Paleontologists and Mineralogists, Pacific Section, p. 51–59.

Rainbird, R.H., Heaman, L.M., and Young, G.M., 1992, Sampling Laurentia: Detrital zircon geochronology offers evidence for an extensive Neoproterozoic river system originating from the Grenville orogen: Geology, v. 20, p. 351–354, doi: 10.1130/0091-7613(1992)020<0351:SLDZGO>2.3.CO;2.

Rainbird, R.H., Jefferson, C.W., and Young, G.M., 1996, The early Neoproterozoic sedimentary Succession B of Northwestern Laurentia: Correlations and paleogeographic significance: Geological Society of America Bulletin, v. 108, p. 454–470, doi: 10.1130/0016-7606(1996)108<0454:TENSSB>2.3.CO;2.

Rainbird, R.H., McNicoll, V.J., Theriault, R.J., Heaman, L.M., Abbott, J.G., Long, D.G.F., and Thorkelson, D.J., 1997, Pan-continental river system draining Grenville Orogen recorded by U-Pb and Sm-Nd geochronology of Neoproterozoic quartzarenites and mudrocks, northwestern Canada: The Journal of Geology, v. 105, p. 1–17.

Reed, B.L., 1968, Geology of the Lake Peters area, northeastern Brooks Range, Alaska: U.S. Geological Survey Bulletin 1236, p. 1–132.

Reiser, H.N., 1971, Northeastern Brooks Range—A surface expression of the Prudhoe Bay Section *in* Proceedings of the geological seminar on the North Slope of Alaska: Los Angeles, California, American Association of Petroleum Geologists, Pacific Section, p. K1–K14.

Reiser, H.N., Dutro, J.T., Brosge, W.P., Armstrong, A.K., and Detterman, R.L., 1970, Progress map, geology of the Sadlerochit and Shublik Mountains, Mt. Michelson C-1, C-2, C-3, C-4 quadrangles, Alaska: U.S. Geological Survey Open-File Report 70-273, scale 1:63,360, 5 sheets.

Reiser, H.N., Norris, D.K., Dutro, J.T., and Brosge, W.P., 1978, Restriction and renaming of the Neruokpuk Formation, northeastern Alaska, *in* Sohl, N.F., and Wright, W.B., eds., Changes in stratigraphic nomenclature by the U.S. Geological Survey, 1977: U.S. Geological Survey Bulletin, p. A106–A107.

Reiser, H.N., Brosge, W.P., Dutro, J.T., and Detterman, R.L., 1980, Geologic map of the Demarcation Point quadrangle, Alaska: U.S. Geological Survey Map I-1133, 1:250,000.

Robinson, M.S., Decker, J., Clough, J.G., Reifenstuhl, R.R., Dillon, J.T., Combellick, R.A., and Rawlinson, S.E., 1989, Geology of the Sadlerochit and Shublik Mountains, Alaska National Wildlife Reserve, northeast Alaska: State of Alaska, Department of Natural Resources, Division of Geological and Geophysical Survey, Professional Report 100, 1:10,000 scale.

Rothman, D.H., Hayes, J.M., and Summons, R.E., 2003, Dynamics of the Neoproterozoic carbon cycle: Proceedings of the National Academy of Sciences of the United States of America, v. 100, p. 8124–8129, doi: 10.1073/pnas.0832439100.

Rowley, D.B., and Lottes, A.L., 1988, Plate-kinematic reconstructions of the North Atlantic and Arctic: Late Jurassic to present: Tectonophysics, v. 155, p. 73–120, doi: 10.1016/0040-1951(88)90261-2.

Saltus, R.W., and Hudson, T.L., 2007, Regional magnetic anomalies, crustal strength, and the location of the northern Cordilleran fold-and-thrust belt: Geology, v. 35, p. 567–570, doi: 10.1130/G23470A.1.

Saltzman, M.R., 2005, Phosphorus, nitrogen, and the redox evolution of the Paleozoic oceans: Geology, v. 33, no. 7, p. 573–576, doi: 10.1130/G21535.1.

Saltzman, M.R., Ripperdan, R.L., Braiser, M.D., Lohmann, K.C., Robison, R.A., Chang, W.T., Shanchi, P., Ergaliev, E.K., and Runnegar, B., 2000, A global carbon isotope excursion (SPICE) during the Late Cambrian: Relation to trilobite extinctions, organic-matter burial and sea level: Palaeogeography, Palaeoclimatology, Palaeoecology, v. 162, p. 211–223, doi: 10.1016/S0031-0182(00)00128-0.

Saylor, B.Z., Kaufman, A.J., Grotzinger, J.P., and Urban, F., 1998, A composite reference section for terminal Proterozoic strata of southern Namibia: Journal of Sedimentary Research, v. 68, p. 1223–1235.

Sengor, A.C., and Natal'in, B.A., 1996, Paleotectonics of Asia: Fragments of synthesis, *in* Yin, A., and Harrison, M., eds., The tectonic evolution of Asia: Cambridge, Cambridge University Press, p. 486–640.

Shields, G., and Veizer, J., 2002, Precambrian marine carbonate isotope database: Version 1.1: Geochemistry, Geophysics, Geosystems, v. 3, p. 1031, doi: 10.1029/2001GC000266.

Shields, G., Deynoux, M., Strauss, H., Paquet, H., and Nahon, D., 2007, Barite-bearing cap dolostones of the Toudeni Basin, northwest Africa: Sedimentary and isotopic evidence for methane seepage after a Neoproterozoic glaciation: Precambrian Research, v. 153, no. 3–4, p. 209–235, doi: 10.1016/j.precamres.2006.11.011.

Smith, D.G., 1987, Late Paleozoic to Cenozoic reconstructions of the Arctic, *in* Tailleur, I., and Weimer, P., eds., Alaskan North Slope geology: Society of Economic Paleontologists and Mineralogists, Special Publication 50, p. 785–796.

Soffer, G., 1998, Evolution of a Neoproterozoic continental margin subject to tropical glaciation [B.A. thesis]: Cambridge, Massachusetts, Harvard College, 99 p.

Stone, D.B., 1989, Paleogeography and rotations of Arctic Alaska—An unresolved problem, *in* Kissel, C., and Laj, C., eds., Paleomagnetic rotations and continental deformation: Norwell, Massachusetts, Kluwer Academic, p. 343–364.

Stone, D.B., 2004, Paleomagnetic paleolatitudes for northeast Russia: An update: American Geophysical Union, Fall meeting, p. GP43C-05.

Summons, R.E., and Hayes, J.M., 1992, Principles of molecular and isotopic biogeochemistry, *in* Schopf, J.W., and Klein, C., eds., The Proterozoic biosphere: A multidisciplinary study: Cambridge, UK, Cambridge University Press, p. 83–93.

Swart, P.K., and Eberli, G.P., 2005, The nature of $\delta^{13}C$ of periplatform sediments: Implications for stratigraphy and the global carbon cycle: Sedimentary Geology, v. 175, p. 115–129, doi: 10.1016/j.sedgeo.2004.12.029.

Sweeney, J.F., 1982, Mid-Paleozoic travels of Arctic Alaska: Nature, v. 298, no. 5875, p. 647–649, doi: 10.1038/298647a0.

Sweeney, J.F., 1985, Comments about the age of the Canada Basin: Tectonics, v. 114, p. 1–10.

Toro, J., Toro, F.C., Bird, K.J., and Harrison, C., 2004, The Arctic Alaska–Canada connection revisited: Geological Society of America Abstracts with Programs, v. 36, no. 5, p. 22.

Urlwin, B., Ayliffe, D.J., Jansyn, J., McKirdy, D.M., Jenkins, R.J.F., and Gostin, V.A., 1993, A $\delta^{13}C$ survey of carbonate in the early Ediacaran Wonoka Formation, *in* Jenkins, R.J.F., Lindsay, J.F., and Walter, M.R., eds., Field guide to the Adelaide Geosyncline and Amadeus Basin, Australia: Australian Geological Survey Organization Record 1993, v. 35, p. 92–96.

Veizer, J., Ala, D., Azmy, K., Bruckschen, P., Buhl, D., Bruhn, F., Carden, G.A.F., Diener, A., Ebneth, S., Godderis, Y., Jasper, T., Korte, C., Pawelleck, F., Podlaha, O.G., and Stauss, H., 1999, $^{87}Sr/^{86}Sr$, $\delta^{13}C$ and $\delta^{18}O$ evolution of Phanerozoic seawater: Chemical Geology, v. 161, p. 59–88, doi: 10.1016/S0009-2541(99)00081-9.

Vogt, P.R., Taylor, P.T., Kovacs, L.C., and Johnson, G.L., 1982, The Canada Basin: Aeromagnetic constraints on structure and evolution: Tectonophysics, v. 89, p. 295–336, doi: 10.1016/0040-1951(82)90042-7.

Walker, J.C.G., and Lohmann, K.C., 1989, Why the oxygen isotopic composition changes with time: Geophysical Research Letters, v. 16, p. 323–326, doi: 10.1029/GL016i004p00323.

Walker, J.C.G., Hays, P.B., and Kasting, J.F.;, 1981, A negative feedback mechanism for the long-term stabilization of the Earth's surface temperature: Geophysical Research Letters, v. 86, p. 9776–9782, doi: 10.1029/JC086iC10p09776.

Wallace, W.K., and Hanks, C.R., 1990, Structural provinces of the northeastern Brooks Range, Arctic National Wildlife Refuge, Alaska: American Association of Petroleum Geologists Bulletin, v. 74, p. 1100–1118.

Whittington, H.B., and Hughes, C.P., 1972, Ordovician geography and faunal provinces deduced from trilobite distributions: Philosophical Transactions of the Royal Society of London, Series B, Biological Sciences, v. 263, no. 850, p. 235–278, doi: 10.1098/rstb.1972.0001.

Witte, W.K., Stone, D.B., and Mull, C.G., 1987, Paleomagnetism, paleobotany, and paleogeography of the Arctic Slope, Alaska, *in* Tallieur, P., and Weimer, P., eds., Alaskan North Slope geology, Volume 2: Bakersfield, California, Society of Economic Paleontologists and Mineralogists, Pacific Section, p. 571–579.

Wright, L.A., Williams, E.G., and Cloud, P.E., Jr., 1978, Algal and cryptalgal structures and platform environments of the late pre-Phanerozoic Noonday Dolomite, eastern California: Geological Society of America Bulletin, v. 89, p. 321–333, doi: 10.1130/0016-7606(1978)89<321:AACSAP>2.0.CO;2.

Yoshioka, H., Asahara, Y., Tojo, B., and Kawakami, S., 2003, Systematic variations in C, O, and Sr isotopes and elemental concentrations in Neoproterozoic carbonates in Namibia—Implications for a glacial to interglacial transition: Precambrian Research, v. 124, p. 69–85, doi: 10.1016/S0301-9268(03)00079-2.

Young, G.M., 1981, The Amundsen Embayment, Northwest Territories: Relevance to the Upper Proterozoic evolution of North America, *in* Campbell, F.H.A., ed., Proterozoic basins of Canada: Geological Survey of Canada Paper 81-10, p. 203–218.

Young, G.M., 1982, The late Proterozoic Tindir Group, east-central Alaska: Evolution of a continental margin: Geological Society of America Bulletin, v. 93, p. 759–783, doi: 10.1130/0016-7606(1982)93<759:TLPTGE>2.0.CO;2.

Zachos, J., Pagani, M., Sloan, L., Thomas, E., and Billups, K., 2001, Trends, rhythms, and aberrations in the global climate 65 Ma to present: Science, v. 292, p. 686–693, doi: 10.1126/science.1059412.

Zhou, C., and Xiao, S., 2007, Ediacaran $\delta^{13}C$ chemostatigraphy of South China: Chemical Geology, v. 237, p. 89–108, doi: 10.1016/j.chemgeo.2006.06.021.

Zhou, C., Tucker, R., Xiao, S., Peng, Z., Yuan, X., and Chen, Z., 2004, New constraints on the ages of Neoproterozoic glaciations in south China: Geology, v. 32, p. 437–440, doi: 10.1130/G20286.1.

Zonenshain, L.P., Kuzmin, M.I., and Natapov, L.M., 1990, Geology of the USSR: A plate-tectonic synthesis: Washington, D.C., American Geophysical Union, Geodynamics Series, v. 21, 242 p.

Manuscript Received 4 January 2008
Revised Manuscript Received 27 April 2008
Manuscript Accepted 27 May 2008

Printed in the USA